AGE RELATED ALTERATIONS OF ADULT NEUROGENESIS AND ASTROCYTES IN ZEBRAFISH *(DANIO RERIO)*

A THESIS SUBMITTED TO

THE GRADUATE SCHOOL OF ENGINEERING AND SCIENCE

OF BILKENT UNIVERSITY

IN PARTIAL FULFILLMENT OF THE REQUIREMENTS FOR

THE DEGREE OF

MASTER OF SCIENCE

IN

NEUROSCIENCE

By

Narin Ilgım Ardıç

September 2019

AGE RELATED ALTERATIONS OF ADULT NEUROGENESIS AND

ASTROCYTES IN ZEBRAFISH (DANIO RERIO)

By Narin Ilgım Ardıç

September 2019

We certify that we have read this thesis and that in our opinion it is fully adequate, in scope and in quality, as a thesis for the degree of Master of Science.

_____

Michelle Marie Adams (Advisor)

_____

Fahriye Duygu Çetinkaya

_____

Urartu Özgür Şafak Şeker

Approved for the Graduate School of Engineering and Science

_____

Ezhan Karaşan

Director of the Graduate School

ABSTRACT

AGE RELATED ALTERATIONS OF ADULT NEUROGENESIS AND ASTROCYTES IN ZEBRAFISH *(DANIO RERIO)*

Narin Ilgım Ardıç

M.Sc. in Neuroscience

Advisor: Michelle Marie Adams

September 2019

Brain aging is marked by a decline in cognitive abilities and associated with neurodegenerative disorders. In order to identify appropriate interventions to change the course of brain aging and age-related neurological disorders, we should first understand the normal age-related changes. Previous studies claimed that there was a correlation between cognitive capacities and number of neurons. However, recent studies have shown no statistically significant change in total neuron number during healthy aging. Therefore, further studies are required to understand the reasons behind these changes in the brain. One possibility could be the age-related alterations in neuronal lineage and glial markers. Thus, this study aims to show the protein levels, distributions, and localizations of key neuronal lineage and glial markers, which include neural progenitor, early neuronal, immature neuron, and mature neuron and glial markers during healthy aging of the zebrafish brain. For this aim, we measured NeuN (Fox-3, Rbfox3, or Hexaribonucleotide Binding Protein-3), MAP-2 (Microtubule-associated protein 2), HuC (ELAV like neuron-specific RNA binding protein 3), DCAMKL-1 (Doublecortin-like kinase 1), and GFAP (Glial fibrillary acidic protein) with immunohistochemistry and western blot techniques. First, the immunohistochemistry technique was applied on two specific proliferation areas, pallium and optic tectum, to detect the changes in the number of neuronal lineages and glial marker. The results indicated no statistically significant changes between young and old groups. Secondly, we performed whole-brain immunohistochemistry of all markers and quantified every image by manually counting the positive signal. We found that aging did not have an effect on the distribution and expression of the markers, even in the whole brain. Finally, Western-blot was performed in whole brain lysates to compare neuron number and protein level changes. Western-blot results indicated an age-related statistically significant decline in immature neuron marker for specifically males and glial marker for specifically females. The protein level of neural

progenitor marker showed the significant decline in males during aging but no change between two age groups. Results of the mature neuron antibody revealed that the protein levels were consistent through aging and did not show variation. Our results overall support the finding that the number of neurons and glia do not change during aging since the numbers of markers were not show statistically significant changes during the aging process in the proliferation areas of the zebrafish brain. However, protein levels showed changes between age and gender groups. Thus, this study shows that understanding changes in the number of cells need to count; protein level is not representative, and zebrafish is an appropriate model for brain aging studies.

ÖZET

ZEBRABALIĞI (*DANIO RERIO*) MODELİNDE YETİŞKİN NÖROGENEZİ VE ASTOSİTLERİN YAŞLANMAYA BAĞLI DEĞİŞİMLERİ

Narin Ilgım Ardıç

Nörobilim Yüksek Lisans Programı

Tez Danışmanı: Michelle Marie Adams

Eylül 2019

Beyin yaşlanması zihinsel yeteneklerin azalması ile belirgin olan ve nörodejeneratif hastalıklarla ilişkisi olan bir süreçtir. Beyin yaşlanması ve yaşlanmaya bağlı nörolojik bozuklukların seyrini değiştirmek ve uygun müdahaleleri belirlemek için önce normal yaşlanmaya bağlı değişiklikleri anlamalıyız. Önceki çalışmalar, bilişsel kapasite ile nöron sayısı arasında bir ilişki olduğunu iddia ediyorken; son çalışmalar normal yaşlanma sırasında toplam nöron sayısında istatistiksel olarak anlamlı bir değişiklik olmadığını göstermiştir. Bu yüzden yaşlanmaya bağlı değişikliklerin arkasındaki nedenlerin anlamlandırılması için yeni çalışmalar gereklidir. Olası nedenlerden birisi, nöronal soy ve glial belirteçlerde yaşa bağlı değişiklikler olabilir. Dolayısıyla, bu çalışmanın amacı, zebra balığı beyninin normal yaşlanmasında nöral progenitör, erken nöronal, olgunlaşmamış nöron, olgun nöron ve glial markerleri içeren anahtar nöronal soy ve glial markörlerin protein seviyelerini, dağılımlarını ve lokalizasyonlarını göstermektir. Bu amaç için immünohistokimya ve Western-blot tekniklerini kullanarak NeuN (Fox-3, Rbfox3 veya Hexaribonucleotide Bağlayıcı Protein-3), MAP-2 (Microtubule ile ilişkili protein-2), HuC (ELAV benzeri nöron-spesifik RNA bağlayıcı protein 3), DCAMKL-1 (doublecortin benzeri kinaz 1) ve GFAP (Glial fibril asidik protein) markerlarına baktık. İlk olarak, iki spesifik proliferasyon alanı olan Pallium ve Optic tectum alanlarında nöronal soy ve glial marker sayılarının değişimlerini tespit etmek için immünohistokimya tekniği uygulandı. Sonuçlar genç ve yaşlı gruplar arasında istatistiksel olarak anlamlı bir değişiklik olmadığını göstermiştir. İkinci olarak, tüm markörler için bütün beyin immünohistokimyasını yaptık ve pozitif sinyalleri manuel olarak sayarak her görüntüyü ölçtük. Yaşlanmanın, tüm beyinde bile belirteçlerin dağılımı ve ifadesi üzerinde bir etkisi olmadığını bulduk. Son olarak, Western-blot tekniğini kullanarak tüm beyin lizatlarında yaşa ve cinsiyete bağlı protein seviyelerindeki farklılıklara hücre sayıları ile karşılaştırma yapmak amacıyla bakıldı. Western-blot sonuçları yaşa bağlı istatistiksel olarak anlamlı

düşüşleri olgunlaşmamış nöronlarda özellikle erkeklerde ve glial markörde özellikle dişilerde gösterdi. Nöral progenitör markörü yaşa bağlı anlamlı bir değişim göstermezken, erkekler için yaşla birlikte önemli bir düşüş gösterdi. Olgun nöron antikorunun sonuçları, protein seviyelerinin yaşlanma ile tutarlı olduğunu ve değişiklik göstermediğini ortaya koydu. Sonuçlar genel olarak, zebra balığı beyninin proliferasyon bölgelerinde yaşlanma süresince markörlerin sayımları istatistiksel olarak anlamlı bir değişiklik göstermediği için, sağlıklı yaşlanma sırasında nöron ve glia sayısının değişmediğini ortaya koymaktadır. Ancak protein düzeyleri yaş ve cinsiyet grupları arasında değişiklikler gösterdi. Bu nedenle, bu çalışma hücre sayısındaki değişiklerin anlaşılabilmesi için hücre sayımının yapılmasının gerekliliğini vurgulayıp, protein seviyelerinin temsili olmadığını ve zebra balığının beyin yaşlanması çalışmaları için uygun bir model olduğunu göstermektedir.

Anahtar Kelimeler: zebrabalığı, yaşlanma, nörogenez, glia, western-blot, immunohistokimya

ACKNOWLEDGEMENTS

TABLE OF CONTENTS

LIST OF FIGURES

LIST OF TABLES

CHAPTER 1

INTRODUCTION

Aging is accepted as the inevitable time-dependent functional decline which is valid for most living organisms [1]. Many of the illnesses or disabilities can be cured or compensated with advanced medicine in our century. However, the aging brain has some unavoidable changes, and research for preventing or decelerating these changes still needs to be done. Brain functions, such as cognition, memory, and learning are reduced with aging which leads to impairment in quality of life.

On the other hand, life span is increasing year after year thanks to the advances in medicine and technology. Average life expectancy has doubled in the last 150 years in most parts of the world [2]. The population aged 65 years and older is predicted to reach 973 million by 2030 [3]. The increasing number of elderly individuals creates an increase in the prevalence of age-related neurodegenerative disorders and cognitive decline. Hence, understanding the underlying mechanisms of healthy aging is the initial step to be taken.

1.1 Age-related Cognitive Decline

Cognitive abilities can be categorized into many domains, which include attention, memory, and executive functions. Each of them represents quantifiable impairment with aging. Amount of decline in the tests also can be explained with increased response time, which depends on age-related decline in perceptional and processing speed [4].

1.1.1 Attention

Attention research reveals noticeable differences with aging. Older adults perform poor performance in complex attentional tasks, especially in divided attention

[5] [6] and selective attention [7] tasks compared with young adults. Divided attention task requires making multiple tasks simultaneously, and selected attention task depend upon ignore irrelevant information while focusing on specific information. On the other hand, the performance of simple attention tasks, like measuring sustained attention does not decline with aging. Instead, it shows improvements in adulthood and then maintains a steady level in aging [8].

1.1.2 Memory

Memory is the first cognitive function that comes to mind when the concept of aging is thought. Memory, as a complex structure, was divided into two main subtypes, short term, and long term [9]. Working memory can be added as the third. This division is based on capacity and memory processes that are involved. Differences between these three types are explained fully in the article by Cowan *et al* [10].

The four stages of memory formation are encoding, consolidation, storage, and recall/retrieval. Encoding is the first step of memory processing. Research indicates an age-related decline in the encoding part [11]. Memory consolidation is the process of stabilization of information after memory acquisition. The following step is storage and can be explained as transferring information to long term memory. Retrieval is recalling information which is encoded recently or previously. Impairments of retrieval are also observed more in older adults comparing to young ones [12].

Two main types of long term memory are declarative (explicit) and nondeclarative (implicit). Declarative memory is a conscious process while nondeclarative is unconscious and effortless. Declarative memory can be analyzed under two subdivisions. Semantic memory is based on factual information, concepts, or general knowledge, while episodic memory includes life experiences or specific

events. Research shows that semantic memory can be preserved during aging until age mid-80s [13]. However, episodic memory shows impairment with aging [14].

1.1.3 Executive Functions

Executive functions are collections of cognitive processes that are required for cognitive control of behaviors to reach the subject's goals. Executive functions include high function cognitive tasks like multitasking, decision making, and planning. All of them require to use more than one cognitive functions simultaneously. Age-related working memory or attention problems cause the decline of executive functioning performance in older ages [5].

1.2 Age-related Biological Changes

All these cognitive disabilities can be accepted as a result of some biological changes. Thus, comprehending biological mechanisms is crucial for getting to the bottom of cognitive decline in aging. Biological changes can be contextualized under two main headings; structural and neuronal.

1.2.1 Structural Changes

Age-related structural changes are observed in parallel with the cognitive changes. Advance in technology and medical science gives the opportunity of imaging structural changes with aging. Many brain structures show age-related alterations like cortical thinning [15], [16].

Grey matter changes can be analyzed with grey matter density in magnetic resonance imaging (MRI). Grey matter density refers to the proportion of voxels from grey matter versus other types of neural tissues. Grey matter density declines with aging as reported in the Sowell and her colleagues' study [17]. Also, age-related increase in white matter lesions, even during normal aging was reported in another MRI study by measuring white matter signal abnormalities [18], [19].

Hippocampus is one of the most studied structure and has a well-known relationship with aging. Hippocampus is accepted to have a role related to memory. Since, one of the most noticeable age-related changes is in the memory, study on the hippocampal alterations becomes crucial. Hippocampal atrophy with aging is mentioned in many studies [20], [21]. Specifically, after the age of 60, volume of the hippocampus shows dramatic decline [22].

1.2.2 Neuronal Changes

During the 70's, it was believed that cortical neurons were lost between 35% and 55% in total from adulthood to old age. Later, researchers recognized that it was an artifact because of the shrinkage differences of old versus young brains during fixation, and that it caused neuronal density differences, not number differences. Recent studies also support insignificant or no loss of neuronal number during normal aging in the whole brain [23]. However, some specific neuron populations like in the hippocampus decline slightly while becoming elder. Understanding the neuronal changes requires a close inspection at the neuronal development and neurogenesis.

1.2.2.1 Neural development

In the general perspective, the nervous system develops in four stages. First, dividing progenitor cells give rise to neurons and glia. Second, these newborn neurons reach axons and dendrites in accordance with their aims. Then, they make synaptic connection with pertinent target cells for starting communication. Lastly, normal neuronal cell death provides to eliminate excessive neurons. Due to this elimination process, synaptic connections change with respect to the pattern of electrical and synaptic activity in the network [24]. After the development, maintenance of neurons and glial cells depend on two basic mechanisms; neurogenesis and gliogenesis.

1.2.2.2 Neurogenesis

Neurogenesis can be explained as the process of forming new neurons in the nervous system. Neurogenesis starts in the embryonic phase when the sufficient number of neural stem cells has been reached and continue in the developmental process in all vertebrates. However, between different vertebrates, it shows differences in the continuity of growth capacity with aging and locational specificity. For instance, in the adult rodent brain limited amount of proliferation were reported in mainly two telencephalic, which are subgranular zone (SGZ) and subventricular zone (SVZ) [25]. Neurogenesis process is completed in these areas with different times in the mammalian brain; 28 days in SVZ and 42 days in SGZ [26].

On the other hand, zebrafish has lifelong cell proliferation in several zones. Figure 1, which was adapted from Kizil et al [27], shows neurogenic areas with stem cell environments from two different species. Neurogenesis is accepted as one of the most remarkable examples of adult neuroplasticity in most vertebrate species [28] and plays a crucial role on the maintenance of cognitive abilities [29],[30] in aging.
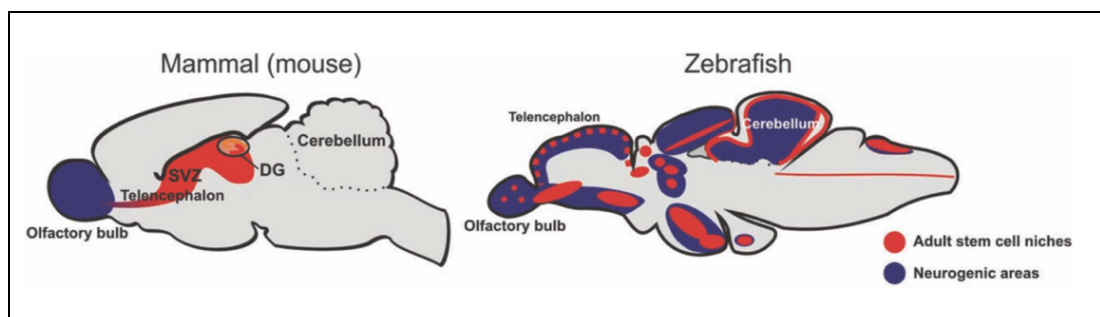
Figure 1.1 Representative image for comparison of neurogenic areas in mammalian brain and zebrafish brain. (Adapted from Kizil et al [27])

Liu and Song [31] describe the adult neurogenesis steps in their review article. In summary, Adult neurogenesis starts with quiescent neural stem cell maintenance and proliferation. After the activation of these stem cells, fate specification happens, and neural progenitors are created in there, and primitive nerve cells or namely,

neuroblasts are produced from them. Next, these proliferating nerve cells exit the cell cycle, and some of them survive as a subpopulation. Differentiation and survival of immature neurons start at this point. Thus, newborn neurons have been created and then, integrated into the existing brain circuit.

Regulation of adult neurogenesis is dependent on some molecular and environmental factors. Many molecular players have an impact on this regulation, like neurotransmitters [32] and growth factors [33]. Environmental factors also have various effects. For example, sleep deprivation causes decreased cell proliferation [34] or, running promotes increasing neurogenesis even in old age [35].

Understanding neuronal changes need to focus on neuronal lineage. Therefore, adult neurogenesis process can be detected by using different neuronal lineage markers, which has some subcategories like progenitor, early neuronal, or immature and mature neuronal markers.

1.3 Neuronal Lineage and Their Corresponding Markers

1.3.1 Markers for Neuronal Progenitors

Progenitor cells can be defined as the cells that have some capacity of differentiating into specific cell types. In previous studies, progenitor cells were considered in the stage between stem cells and mature cells. Researchers have accepted the progenitors and stem cells as two distinct cells by their features of them; progenitors being unipotent or oligopotent, whereas stem cells being multipotent [36]. However, recent understanding states that the progenitor cells are stem cells with limited differentiation ability without strict classification [37]. Progenitor cells may be accepted more specific type of stem cells with limited capacity of maintaining self-renewal while stem cells have unlimited maintaining capacity. Limited potency of progenitor cells makes them more narrow then the stem cells. Thus, progenitor cells

are divided into many different subtypes according to their purposes. Afterwards, differentiation of them to the post-mitotic immature neurons initiates the migration to final destination of these progenitor cells.

1.3.1.1 Doublecortin and Doublecortin-like Kinase-1

Doublecortin (DCX) is a microtubule-associated protein and one of the most commonly used neural progenitor marker in mammalian species [26]. DCX is expressed during the development of neuroblasts and also a marker of migrating neuroblasts [38]. Doublecortin-like kinase-1 (DCAMKL-1) have 80% amino acid similarity with doublecortin protein and additionally DCAMKL-1 can play a similar role with Microtubule-associated proteins (MAPs) [39]. Lin and his colleagues indicated that the expression pattern of DCAMKL-1 is overlapping with DCX [40]. Their study also showed that the DCAMKL-1 with DCX in other species can be substituted. Moreover, the homology of DCAMKL-1 and DCX is proven some older studies [41], [42]. Another more recent study also indicated that DCAMKL-1 can be used instead of DCX in zebrafish model organisms [43].

1.3.2 Markers for Immature Neurons

Immature neurons are created from neuroblasts, which are derived from different types of neuronal progenitors. They lost the dividing ability and will have to migrate to the final destination to transform mature neurons. Thus, differentiation occurs in this phase.

1.3.2.1 Elav like neuron-specific RNA binding protein 3

Elav like neuron-specific RNA binding protein 3 (HuC) is expressed in all neurons immediately after the birth. Thus, it is commonly used for marking immature neurons in mammalians and teleost species. HuC is a counterpart of drosophila Elav

like neuron-specific RNA binding protein 3 in vertebrates [44], [45]. HuC plays a role in neuronal differentiation and determination of fate with other Hu proteins [46].

1.3.3 Markers for Mature Neurons

Mature neurons are already differentiated and lost the ability of dividing. The function of mature neurons can be explained as taking part in all information steps, which include receiving, processing, and transferring all over the information in nervous systems.

1.3.3.1 Neuronal Nuclear Antigen

Neuronal nuclear antigen (NeuN) is the most frequently used mature neuron marker in all vertebrates. It is expressed in almost all postmitotic neurons while it is absent outside the nervous system. However, it shows rare exceptions also in some neural cell types. Expression in Purkinje cells, photoreceptor cells, and mitral cells were mentioned as negative when it was explored in the early nineties [47]. Moreover, recent studies indicated that there is no expression in the substantia nigra, especially in dopaminergic neurons [48], [49]. On the other hand, using NeuN as differentiated mature neuron marker is advantageous with specificity on only mature neurons, and association with cell nucleus rather than cytoplasm which means that NeuN detection can be easily quantified [50].

1.3.3.2 Microtubule-Associated Protein -2

Microtubule-Associated Protein -2 (MAP2) is one of the major members of the microtubule-associated protein group. They are expressed in all vertebrates and used as a mature neuron marker. MAP2 stabilizes soma and microtubules in the dendrites of mature neurons while playing a role in dendrite generation [51]. Another function of MAP2 is being the scaffolding protein in the nervous system [52]. It also plays a

role in synaptic plasticity due to its function in the dendrite formation [53]. Sanchez *et al.* were explained MAP2 function in their well-documented review article [54].

1.4 Glia

Glia can be defined as nonneuronal cells in central nervous systems (CNS) and play a role as a supporter of neurons in many ways. Gliogenesis occurs in a similar way to neurogenesis. Glial cells have three main types in the CNS, which are microglia, oligodendrocytes, and astrocytes.

1.4.1 Microglia

Microglia amounts to almost 10% of the central nervous system [55] and takes role in many mechanisms like hemostasis and development. The main contribution of microglia to CNS is immunity. Neuroinflammatory responses are mediated by microglia in there. Microglia also plays a crucial role in some synaptic mechanisms like synaptic pruning which is an essential step in development of the nervous system and continues with aging [56], and synaptic plasticity [57] which can be explained as alteration of synapse strength between two neurons and play role on learning and memory [58]. Age-related changes like decreasing arborized area of microglial cells are observed, especially in pathological aging [59]. However, more studies will be needed to clarify whether microglia are responsible for neurodegeneration with aging or whether aged neurons itself are more apt to degenerative cues [60]. Recently published review paper of Butovsky and Weiner explained the role of microglia in health and disease thoroughly [61].

1.4.2 Oligodendrocytes

Oligodendrocytes are the dominant glial cells in white matter [55]. They play a vital role in the formation of the myelin sheath around the axons in the nervous system. Myelin sheath has a unique composition with rich content of lipids, and low

water content, and this composition allows the electrical insulation of axons. Segmental structure of myelin sheaths is responsible for saltatory conduction of nerve impulses. Myelin sheaths provide fast conduction enable, accurate signal in long distance and space economy [62]. Myelin sheaths in CNS are mostly located in white matter. Age-related changes of oligodendrocytes are observed in white matter. Studies indicated that degeneration of oligodendrocytes and their progenitor cells cause an increase in myelin breakdown. Naturally, it causes decrease in remyelination and inevitable distortion of white matter integrity during aging [63], [64]. Another essential role of oligodendrocytes is to secrete some neurotrophins and create local trophic support for neurons [65]. Lee and colleagues reported that abnormality of oligodendrocytes leads to axonal degeneration [66], which is observed in normal and pathological aging [67].

1.4.3 Astrocytes

Astrocytes are one of the best studied glial cells in CNS. Astrocytes create approximately 20% to 40% of total brain cells of the mammalian brain [68]. They have crucial functions to maintain many mechanisms in CNS such as, structural formation, metabolic support, and synaptic regulation. Astrocytes also have significant interactions with other CNS glial cells. They promote blood flow and oxygenation locally by contributing neurotransmitter release. Their end foot processes wrap blood vessels and control vessel diameter by playing the role of potassium ions release and hyperpolarization of smooth muscle cells [69]. Also, they play a role in the energy metabolism of the brain by taking up glucose from the blood and converting it to lactate. Then, released lactate, provides local energy for neurons [70], [71]. Another function of astrocytes is the homeostasis of some ions like potassium, chloride, sodium, and hydrogen [72], [73]. For example, controlling ion and water homeostasis

through an astrocytic water channel (aquaporin-4), which eventually affects on brain plasticity [74] and volume [75].

Astrocytes are also one of the key glial cells for synaptic formation, elimination and, as a result of these, plasticity. Ullian and his colleagues have used highly purified cultures of retinal ganglion cells by adding astrocyte conditioned medium to show the role of astrocytes on synapse formation and observed that astrocytes induced the development of vast numbers of synapses [76]. Besides, astrocytes contribute activity-dependent synapse elimination via Multiple epidermal growth factor like domains protein 10 (MEGF10) and c-mer proto-oncogene tyrosine kinase (MERTK) pathways in developing and adult CNS [77]. Astrocytes have a relationship with other types of glial cells in CNS. Their relationship manifests impacts with aging. Liddelow and his colleagues showed that astrocyte activation is highly correlated with released reactive microglia and also, the same study indicated that astrocytes produce some neurotoxic factors which may damage neurons and oligodendrocytes even in the normal aging [78].

1.4.3.1 Glial Fibrillary Acidic Protein

Glial fibrillary acidic protein (GFAP) is a member of intermediate filament proteins and expressed in some cell types which include mainly astrocytes in CNS. GFAP is a major component of astrocyte cytoskeleton. Thus, it is one of the widely used markers for astrocyte determination [79]. GFAP shows high expression in amyloid plaques in Alzheimer disease, and many studies indicated that this high expression depends on the reactive astrocytes [80],[81],[82]. Moreover, GFAP and intermediate filament system of astrocyte are accepted to be highly correlated with many other CNS diseases [83]. Nowadays, GFAP transgenic model organisms are

frequently used for these reasons [84], [85]. Also, GFAP plays a role as a neuronal progenitor marker because of the expression in early radial glia. They are accepted as a member of type 1 hippocampal progenitors [86], [26]. They have a function on neuroblasts and neurons for giving rise [87].
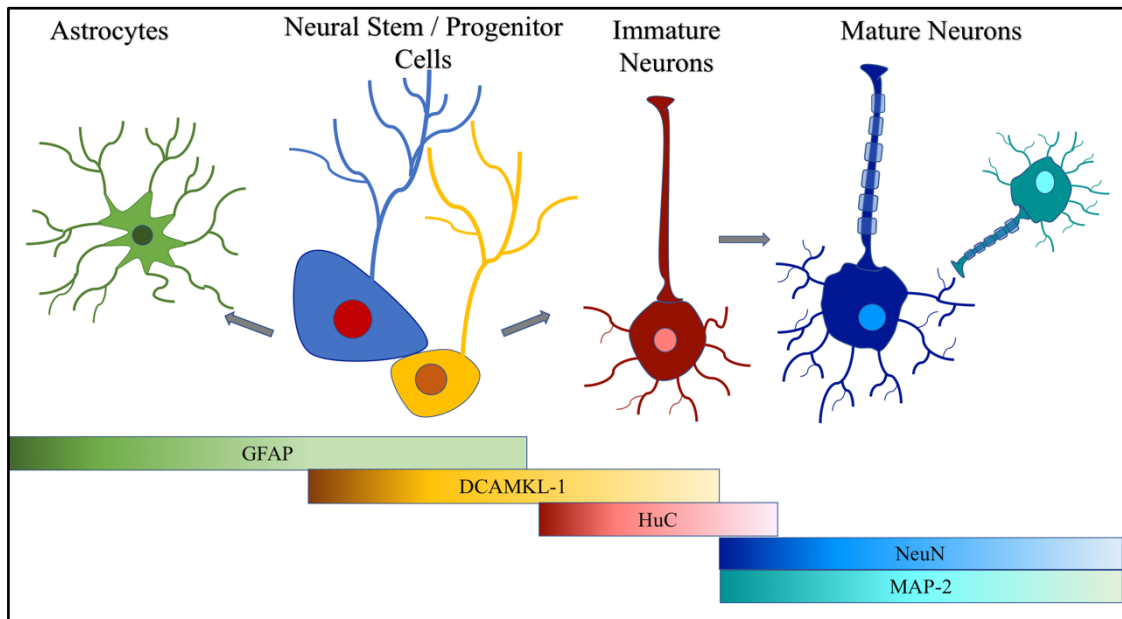
Figure 1.2 Representative image for neural lineage and their corresponding markers in this study. Representative drawings show related cells in the top of the image. Rectangular blocks refer corresponding markers of them.

1.5 Age-Related Sexual Dimorphism

Gender differences are became apparent with aging at the some areas like behavioral, structural, and in the molecular level. Behavioral changes are demonstrated differently in the ability level; males show better results than females in motor and spatial abilities while females are better at memory and social cognition tasks than males. Functional MRI and other imaging techniques were used to find the reason

behind these differences in many studies. However, more research is required to find the relationship between aging and sexual dimorphism.

A recent study indicated sexual dimorphism in human brains based on blood flow by using single photon emission computed tomography while participants perform the task while they are in resting state. Amen *et al.* found that females have more activation in the prefrontal cortex and limbic areas compared to males, whereas males have more active visual and coordination center then females [88].

Changes in the structural and molecular level changes can be accepted as the underlying reason for cognitive alterations with gender. Goldstein and his colleagues showed sexual dimorphism in cortical and subcortical level. Their study mentioned sexual dimorphism in cortical volumes. In detail, females have a larger amount in frontal and medial paralimbic cortices while males have larger volumes in frontomedial cortex, amygdala, and hypothalamus. This comparison was based on relativity on cerebrum size in their study [89]. Also, studies were indicated that males have a higher volume of white matter than females [90].

In the neuronal level, the impact of gender differences can be observed in many areas. In the mammalian brain, adult neurogenesis shows gender differences in dentate gyrus as that female animals display higher newborn neurons [91]. These differences can be explained at the level of sex hormones. In a general perspective, Estrogen provides more proliferation advantage while androgens are increasing the survival of neurons. Mahmoud *et al.* describe impact of sex hormones on neurogenesis in the well-documented review article in detail [92].

1.6 Zebrafish as a model organism

Zebrafish (*Danio rerio*) is one of the most popular model organism in developmental and biological studies. Zebrafish provides many advantages. First of all, zebrafish genome shows significant similarity with human genome. Zebrafish genome has at least one orthologue for the 70% of human genes [93]. Also, zebrafish has a high fertility rate; one pair of zebrafish produce hundreds of embryos with weekly intervals. Maintenance of zebrafish is easier and cheaper than many model organisms. Also, this species has transparent embryos, which provide easy manipulation and observation of development. These advantages made zebrafish famous for a wide variety of disease research [94]. In addition to these advantages, adult zebrafish have an integrated a nervous system like mammals. Having an integrated nervous system ensures a homologous brain and structure with human.

Zebrafish brain development shows some similarities with mammalian brain development. Consequently, zebrafish and human brain have morphological similarities. On the other hand, telencephalon and optic tectum development show differences starting with the embryonic stage [95], [96].

The telencephalon follows eversion way to reach out dorsally in the embryonic stage. This process made it difficult to find homologs of telencephalic regions like hippocampus in mammalian brain in previous researche. However, currently, we have detailed information the accurate location and homologs of the telencephalic regions in the zebrafish brain. The zebrafish telencephalon can be divided into two parts; pallium, which is the dorsal part, and sub-pallium, which is the ventral part [97]. In the mammalian brain, researchers consider hippocampus, amygdala, and basal ganglia as main structures of the telencephalon. In the zebrafish, subdivisions of pallium represent these areas [98]–[100].

Optic tectum is one of the other apparent regions which has a developmental difference in locationally. Teleost species have a dominant structure of optic tectum in the mesencephalon. Zebrafish, as one of the teleost species, also shows this dominance. Optic tectum can be accepted as a visual center in zebrafish brain like other teleost and corresponds to the superior colliculus in human midbrain. Optic tectum is one of the vital processing areas of sensory information with the advantage of having connections with diverse other regions. Acquired visual information is integrated with motor information for generating suitable behavioral responses in the optic tectum. Optic tectum is formed by six different layers; stratum marginale, stratum opticum, stratum fibrosem et griseum superficiale, stratum griseum centrale, stratum album centrale, and periventricular zone [101]. The periventricular zone is a significant region for having most of the neurons of optic tectum. Studies indicated that the periventricular zone has identifiable cell proliferation in adult zebrafish [102]. Optic tectum plays a significant role to prove that proliferating cells continue in to the rostrocaudal axis of zebrafish in aging as well [102], [103].

The life span of zebrafish can be exceeded up to 5 years in the laboratory conditions, which is much longer than other common model organisms [104]. Also, age-related alterations similar with humans can be observable in zebrafish [105]. Age-related cognitive decline is one of the parallelism with humans. Many different cognitive performance tasks can be applied to zebrafish [106]. Zebrafish shows parallel performances in this cognitive function tasks with humans like the decline of spatial memory and learning performances with aging [107]. Biological changes are also observing as an underlying mechanism of gradual cognitive decline. Oxidative stress [108], decreased neurogenesis [109], and shortened telomeres[110] are some of

these age-related biological changes. In light of this information, zebrafish can be accepted as a useful model organism for gerontological studies.

1.7 Aim of This Thesis Study

Brain aging is marked by a decline in cognitive abilities, which includes attention, memory, and executive functions. First, understanding changes in healthy aging is crucial for identifying proper interventions to age-related neurological disorders. Previous studies claimed that there was a correlation between cognitive capacities and number of neurons. On the other hand, recent studies showed that neuron number is not decreased with aging in most of the species which is contradictory of the old belief. Thus, further research needs to focus on underlying mechanisms of neuron numbers or the other possible players. For this aim, this research was focused on neural lineage and glial changes during aging with using zebrafish (*Danio rerio*) model organism. Protein levels, distributions, and locations of target markers, which are neural progenitor, immature and mature neuron, and astrocyte were detected with using Immunohistochemistry and Western-blot techniques. The immunohistochemistry experiments were focused on two specific proliferation areas which are the Pallium and Optic Tectum, and also whole brain measurements, and were made for comparing with protein levels. Western-blot techniques were applied to the whole brain because the sizes of the target areas are not suitable for extracting protein individually and pooling them has the potential to lose biological differences.

CHAPTER 2

METHODS

In this study, two different methods, Western Blot and Immunohistochemistry were used to show the intensity and morphological location of selected proteins.

2.1 Subjects

All fish were maintained in the Bilkent University Molecular Biology and Genetics Department Zebrafish Facility. The facility is using a standard system which built by ZebTec Zebrafish Housing System (Tecniplast, Italy). The system keeps the temperature of water at 28 °C and maintains the pH between 7.0-7.5. Water quality was checked with readings of the mechanical and carbon filters every day. Animals were maintained either in 3.5 L or 8L tanks with a 14-h light:10-h dark cycle. Fish were fed dry flakes (twice times) and fresh artemia (once time) every day. All the animals in this part come from the TgBAC (gfap-GFP) zf167 transgenic line, which was obtained from the European Zebrafish Resource Center and was fed and maintained by us.

Bilkent University Local Animal Ethics Committee (HADYEK) approved the animal ethics protocols of this study with approval dates & numbers: July 10, 2015, & 2015/31 and February 21, 2018, & 2018/4. Animal distributions are illustrated in the Table 1 and Table 2 for western blot experiments and immunohistochemistry experiments respectively. Young animals were 7 to 9 months old. Old animals were 33 to 42 months old.

2.2 Euthanasia

Ice-water was used to euthanise all the animals. The small plexiglass holding the tank was filled with system water up to half, and ice was added until the

temperature was between 4-7°C. Fish were transferred to the tank and remained there until no gill movements were observed.

Table 2. 1 Number of animals that were used for Western Blot experiments

WB	Female	Male
Old	7	9
Young	9	7

Table 2.2 Number of animals that were used for Immunohistochemistry experiments

IHC	Whole brain	Area specific
Old	2	4
Young	2	4

2.3 Western Blot

2.3.1 Dissections

Heads were decapitated from the body with scalpel blade after euthanasia. The crown was placed as dorsal side downwards under the stereomicroscope. Gills were removed and taken aside. Other connective tissues were removed until reaching the skull and the optic chiasm, is exposed. Connectivity of optic chiasm between one of the eyes was cut off. Then, the eyes were removed and transferred into another plate. Skull was cracked open carefully, and the brain was checked from the ventral side whether it is intact or not. Then, it was extracted carefully and checked again for the presence of all brain structures. After the extracting brain, gills, eyes, and brain were put into 1.5 ml eppendorf tubes, weighed quickly, and snap frozen immediately. Snap freezing made by using liquid nitrogen to avoid further degradation. Gender determinations were made by opening peritoneal cavity and by observing the presence

of eggs or testis. After gender determination, bodies were also snap frozen, and all samples were stored -80°C until the protein isolation.

2.3.2 Protein Isolation from the Whole Brain of the Zebrafish

Radioimmunoprecipitation assay (RIPA) buffer [50-mM Tris-HCl, pH 8.0, containing 150mM NaCl, 1% NP-40, and 0.1% SDS and protease inhibitor (2× stock, catalog number: 05 892 970 001, Roche)] was prepared according to Table 3 as lysis buffer to lysate target proteins in the whole cell. Tissues were taken from -80°C and put into previously prepared RIPA buffer according to weight of the tissue. Approximately 60 µl buffer was added for each 1 mg of tissue.

Table 2. 3 Recipe of RIPA buffer

Stock solution	Amount (µl)
2M NaCl	75
1M Tris-HCl pH:8	50
NP-40 (100%)	10
SDS (10%)	10
ddH$_2$O	355
Protease Inhibitor (2x)	500

Tissues, which were immersed in RIPA buffer, were homogenized with a 25-gauge, 2mL syringe by pawing through 10 times in the 1,5 ml eppendorf tubes on ice. Homogenates were incubated on ice for 30 minutes, mixing every 10 minutes gently. At the end of the 30 minutes, homogenates were centrifuged at 13,000 rpm for 20 minutes at 4°C. Supernatants were collected, aliquoted, and stored at -80°C until the measurement of soluble protein concentration with Bradford Assay.

2.3.3 Bradford Assay

The concentration of soluble proteins was determined by using 96 well plate in Bradford assay. First of all, ddH_2O, standards, and samples were loaded in order. Blanks include only ddH_2O. Standards included bovine serum albumin (BSA, Catalog Number: A7906, Sigma-Aldrich, St. Louis, MO, USA) ranging from 2-20 µg/ml and ddH_2O. Detailed information of standards is given in Table 2.4. Samples include 0.5 µl isolated proteins and 4.5 µl ddH_2O. All measurements were done in duplicates. Representative plate template can be seen in Table 2.5. The total volume of each well was 5 µl after adding ddH_2O, BSA standards, and protein samples. 250 µl of Bradford Reagent (B6916, Sigma, St. Louis, MO, USA) was added into each well. A 96-well plate was mixed on an orbital plate shaker at 300 rpm at room temperature for 2 minutes. Aims of the step are mixing them completely while minimizing possible air-bubbles from loading part. After shaking, the plate was incubated in room temperature for an extra 10 minutes without any agitation. Air-bubbles were checked one more time, and if wells have them, they were popped by using sterile syringe tip because each of them has the potential to impact the absorbance values of the samples. Measurement of absorbance values was made with using a multi-plate reader (SpectraMax M5, Molecular Devices, Sunnyvale, CA, USA) at 595 nm. Blank wells assignment were made before starting measurement for subtracting from absorbance values of each other wells which filled with standards and samples. Net absorbance of the standards and concentrations of them were used to calculate the concentration of protein samples by plotting and applying a linear curve fit on these data points and reaching the standard curve.

Table 2. 4 Preperation of standards for Bradford Assay

	ddH$_2$O (µl)	BSA (µl) (1mg/1ml stock)	Final Conc. (µg/µl)
Blank	5	0	0
Standard 1	4.5	0.5	0.1
Standard 2	4	1	0.2
Standard 3	3	2	0.4
Standard 4	2	3	0.6
Standard 5	1	4	0.8
Standard 6	0	5	1

Table 2. 5 Respresentative 96-well plate design for Bradford Assay

	1	2	3	4
A	Blank	Blank	Sample 1	Sample 1
B	Standard 1	Standard 1	Sample 2	Sample 2
C	Standard 2	Standard 2	Sample 3	Sample 3
D	Standard 3	Standard 3	Sample 4	Sample 4
E	Standard 4	Standard 4	Sample 5	Sample 5
F	Standard 5	Standard 5		
G	Standard 6	Standard 6		
H				

2.3.4 Sodium Dodecyl Sulfate–Polyacrylamide Gel Electrophoresis (SDS-PAGE)

SDS-PAGE was used to separate proteins according to their sizes. Two types of SDS-PAGE gel were used for this aim; 10% resolving (pH 8.8) with high acrylamide content and 5% stacking (pH 6.8) which is composed of low acrylamide proportion.

2.3.5 Preparation of Resolving and Stacking Gel

Two different sized glass plates, one of them has an integrated spacer of 1.5 mm (Biorad Life Science 1000 Alfred Nobel Drive Hercules, California 94547 USA) and one 1.5 mm thick comb with 15 well or 10 wells (Biorad Life Science 1000 Alfred Nobel Drive Hercules, California 94547 USA) were used to prepare for each gel. Glass plates were attached to each other and placed in to casting stand.

A 10% resolving gel was made according to the order given in Table 2.6. After adding last reagent, the gel was mixed well gently and poured quickly between the glass plates with pasteur pipette. 2-propanol was added immediately to eliminate the air bubbles in the resolving gel. After the polymerization was observed, 2-propanol was washed out, and the surface of the resolving gel was rinsed with ddH$_2$O and blotted with whatman papers.

Table 2. 6 Recipe of 10 mL 10% Resolving Gel

Order	Substance	Amount (ml) (for 10ml)
1	ddH$_2$O	4.8
2	1.5 M Tris (pH=8.8)	2.5
3	10% SDS	0.1
4	40 % Bis-Acrylamide	2.5
5	10% APS	0.1
6	TEMED	0.01

A 5% stacking gel was prepared by using the reagents in the Table 2.7 and adding them according to the given order in Table 2.7. Substances were mixed slowly and poured by using Pasteur pipette above the polymerized resolving gel, and the related comb was placed on it. After polymerization occurred, the gel was located in to the tank with a holding apparatus for loading and running steps.

Table 2. 7 Recipe of 5% Stacking Gel

Order	Substance	Amount (ml) (for 8 ml)
1	ddH$_2$O	4.824
2	0.5 M Tris (pH=6.8)	2.0
3	10% SDS	0.08
4	40 % Bis-Acrylamide	1
5	10% APS	0.08
6	TEMED	0.016

2.3.5.1 Solutions

1.Resolving Buffer (1.5 M Tris-HCl, pH 8.8):

18.171 g of Tris Base (FW:121.14) was dissolved in 50 ml of ddH$_2$O. Then, pH was adjusted to 8.8 with HCl then filled with ddH$_2$O up to 100 ml.

2. Stacking Buffer (0.5 M Tris-HCl, pH 6.8):

6 g Tris Base (FW:121.14) was dissolved in 60 ml ddH$_2$O. Then, pH was adjusted to 6.8 with HCl then the volume was adjusted as 100ml with adding ddH$_2$O.

3. Sodium Dodecyl Sulfate SDS (10%):

10 g lauryl sulfate was dissolved in 90 ml ddH$_2$O dissolve, brought to 100 ml. SDS is a powerful irritant, so it was handled in toxic hood.

4. Ammonium per sulfate APS: (10%):

30 mg ammonium per sulfate was dissolved in 300 μl sddH$_2$O.

2.3.6 Preparing, Loading and Running of the Protein Samples

Samples were diluted according to the concentration required for the antibody to function properly and Bradford Quantification assay values in the loading buffer in

the related size Eppendorf tubes. Samples were incubated at 95°C for 10 minutes. Then, they were quick spinned and put on ice until loading the SDS- PAGE gels.

Gels of 1.5 mm thickness were cast and run in Mini-PROTEAN Tetra Cell Electrophoresis system (BioRad, CA, USA). Glasses were placed on cassette which was located into the tank. The tank was loaded with 1 x Running buffer up to 2 gel-level. The comb was removed from the stacking gel carefully, and wells were washed with 1 x Running buffer. Samples and prestained protein ladder was loaded into the wells with fine pipette tips avoiding any air-bubbles into the wells. Thermo Scientific PageRuler Prestained Protein Ladder (2x250 µL 10 to 250 kDa- with product number 26619) was used for determining the molecular weights of samples and target proteins in each gel. The tank was connected to power supply (BioRad, CA, USA) and gels were started to run at 90 V in room temperature for 30 minutes. After samples reached to resolving gel level, the running voltage was altered to 120 and continued to run until the adequate separation was observed. Average running time was 120 minutes.

2.3.6.1 Solutions:

1. **2x Loading Buffer:**

Loading buffer was prepared according to the Table 2.8, and 10% DTT was added freshly before each time.

Table 2. 8 Recipe of 2x Loading Buffer

Stock Solution	Amount (ml)
10% SDS	4
20% Glycerol	2
4% BPB	0.1
0.125-M Tris, pH 6.8	2.5

2. 10x Running Buffer:

Table 2.9 shows the materials for 10x Running buffer and before adding the related amount of water pH adjusted to 8.3. Before starting to each experiment, 1x Running buffer prepared by dilution from 10 x Running buffer.

Table 2. 9 Recipe of 10x Running Buffer

Materials	Amount (For 1L)
250 mM Tris	30.285 g
1.9 M Glycine	144.134 g
10% SDS	100 ml
ddH$_2$O	Up to 1 L

2.3.7 Transfer

After the running end, gels were removed from electrophoresis chamber. Glass holders were separated from each other, and stacking gels were removed from resolving gel. Then, resolving gels were put into the 4°C transfer buffer to equilibrate. Transfer step relays on the transferring the proteins in the gel to the membrane by using electric field. PVDF membrane (Immubilon-P Transfer Membrane MD Millipore, Billerico, MA, USA), and whatman filter papers were cut according to related dimensions. Membranes were cut as being the same size as gel which is 6 x 9 cm and whatman filter papers size arranged according to sponge supplied with system kit, which is 8 x 10 cm. PVDF membrane was rinsed in 100% methanol (MeOH) for 45 seconds and incubated in 4°C transfer buffer for 5 minutes. All other material of transfer system, which are 2 sponges, and 4 whatman filter papers for each gel were soaked in the 4°C transfer buffer. Transfer sandwich was prepared in the following order: First, Mini Trans-blot Electrophoretic Transfer Cell module (BioRad, CA, USA) located to the black surface of the plastic holder at the bottom, and one sponge

was located on it. Then, 2 pieces of whatman filter paper were placed on it, and SDS-PAGE gel put on their center. PVDF membrane was located as covering gel completely. Two whatman filter papers put and air bubbles were removed with rolling 15 ml falcon. Finally, the sponge was positioned into them, and the sandwich module closed. In each of the steps, transfer buffer was added to avoid drying. Closed Plastic holder located in to transfer cassette with checking the color codes for detecting electrode sides to allow segregated proteins transfer from SDS-PAGE gel to PVDF membrane. The power supply was changed to 100V for 90 minutes, and the transfer was performed in cold room to eliminate increasing the current milliampere.

2.3.7.1 Solution

1. **Transfer Buffer:**

Transfer buffer was prepared with using materials with related amounts in the table 2.10 before adding the methanol, Tris, and glycine were dissolved in water. After preparation, the buffer was stored in 4 ^{o}C.

Table 2. 10 Recipe Transfer Buffer

Materials	Amount (For 2L)
25-mM Tris	6g
195-mM Glycine	28 g
ddH$_2$O	Up to 1.6 L
Methanol	400 ml

2.3.8 Blocking and Primary & Secondary Antibody Incubation

After the transfer finished, the plastic holder was opened, and PVDF membranes were taken and put into one-hour blocking buffer incubation at room temperature on a shaker. Blocking buffer was prepared according to information from

optimization experiments of selected antibodies. Blocking buffers were prepared in Tris Buffered Saline with Tween 20 (TBS-Tween) buffer with non-fat milk powder or bovine serum albumin (BSA) (Sigma-Aldrich, St. Louis, MO, USA). Blockings were made for 1 hour in room temperature with gentle agitation. After the 1 hour, primary antibody incubations were made. For western blot part, five different primary antibodies were used. Anti-NeuN (Abcam, Cambridge, UK: ab177487, 1:2000 dilution), anti-HuC (Abcam, Cambridge, UK: ab78467, 1:500 dilution), anti-DCAMKL-1 (Abcam, Cambridge, UK: ab109029, 1:1000 dilution), anti-GFAP (Abcam, Cambridge, UK: ab53554, 1:1000 dilution) and anti-β tubulin (Cell Signaling Technology, Danvers, AM, USA: #2146, 1:5000 dilution) were primary antibodies in this study. Anti-β tubulin was used as an equal loading control. Anti-NeuN and anti-GFAP antibodies were prepared in block solution: %5 BSA while the others, anti-HuC, anti-DCAMKL-1, and Anti-β tubulin were preparing in the block solution: 5% non-fat milk powder. Recipes of blocking solutions were given in the following solutions part. Primary antibody incubations were made in cold room for 17 hours with a rocking motion.

Membranes were taken out from the cold room. Primary antibodies were collected and stored at -20 $^{\circ}$C for reusing. Membranes were washed with TBS-Tween for five times at room temperature with a rocking motion. Duration of washings were 5, 5, 10, 5, 5 minutes for Anti-Huc, anti-DCAMKL-1, anti-GFAP, and Anti-β tubulin. However, for anti-NeuN, extra two washings 10 and 5 minutes were added to reach clear band images with minimizing nonspecific boundings.

After the washings, horseradish peroxidase (HRP) conjugated secondary antibody selected and prepared related to primary bodies raised species and blocking

solution preferences. DCAMKL-1, HuC, anti- NeuN and Anti-β tubulin were raised in rabbit. Anti-rabbit-HRP (Cell Signaling Technology, Danvers, AM, USA: #7074, 1:5000 dilution) was used as a secondary antibody for those primary antibodies. Anti-goat- HRP (abcam, Cambridge, UK: ab97100, 1:10000 dilution) was used as a secondary antibody for anti-GFAP. Secondary antibodies for NeuN and GFAP were prepared in Blocking Solution: 5% BSA while the others prepared in Blocking Solution: 5% non-fat milk powder. Secondary antibody incubations were done on the shaker for 1 hour at room temperature.

After, secondary antibody incubation over, seven washings for NeuN and five washings for others were made with using TBS-Tween at room temperature on shaker like washings after the primary antibody incubation.

2.3.8.1 Solutions

1. **10 X Tris-Buffered Saline:**

10 x TBS buffer was prepared according to table 2.11. Volume was completed to 1L after the pH was adjusted to 7.6 with 1 N HCl/ NaOH.

Table 2. 11 Recipe of 10x Tris-Buffered Saline

Materials	Amount (For 1L)
100 mM Tris	12 g
1.5 M NaCl	88 g
ddH$_2$O	Up to 1L

2. **Tris-Buffered Saline and Tween 20 (TBS-Tween):**

3 mL of Tween-20 was added to 1 L of 1X TBS.

3. **Blocking Solution: 5% Non-Fat Milk powder (Stock)**

2.5 g milk powder was dissolved in the TBS-tween as final volume became 50 ml via using vortex.

4. **Blocking Solution: 5% BSA (Stock)**

2.5 g BSA was dissolved in the TBS-Tween as final volume became 50 ml via using vortex.

Table 2. 12 Antibody information for Western Blot experiments

Antibody Name	Specifications	Dilution	Blocking	Secondary antibody
NeuN	Mature Neuron	1:5000	In BSA	Anti-rabbit HRP
HuC	Immature Neuron	1:100	In milk powder	Anti-rabbit HRP
GFAP	Progenitor & Glial Cells	1:1250	In BSA	Anti-goat HRP
DCAMKL-1	Progenitor Cells	1:300	In milk powder	Anti-rabbit HRP
β Tubulin	Equal Loading	1:5000	In milk powder	Anti-rabbit HRP

2.3.9 Chemiluminescent Detection

Chemiluminescent detection was made using Supersignal West Femto Maximum Sensitivity Substrate (Thermoscientific, Rockford, IL, USA: 34095). This kit includes two components, which are Luminol/Enhancer solution and Stable peroxide solution. Solutions were mixed with equal amounts (1:1 ratio), and then membranes were put on a clean surface. Bands of interests which determined according to marker were covered with mixed buffer. 5 minutes of incubation was made in the dark chamber. ChemiDocTM XRS+ imaging system (Biorad, CA, USA) with the ImageLab software (Biorad, CA, USA) was used for imaging.

2.3.10 Image Quantification

All images which were exported from ImageLab software were quantified with ImageJ software (NIH, Bethesda, MD, USA). First, images were converted to 8-bit from the RGB scale. The interested bands from each sample were selected separately with the rectangular selection tool. Each band area were selected to be the same sized rectangular. After the selection of each line of the cohort was done, selected areas were plotted. The space between the two peaks was drawn and chosen to be measured. An independent researcher, Bilge Aşkın, made re-labeling of images for avoiding the possible bias of quantification.

Two different normalizations were made on the data obtained from ImageJ. First, within-gel normalization was performed. Within gel normalization aimed to reach normalized values by eliminating differences of exposure and interassay. The necessity of within gel normalization depends on at least two technical replicas were performed for each of the samples. Normalization was made with following steps; the intensity of the selected band was divided to the average of all bands of the same blot cohort in the same gel. This normalization was applied to each protein of interest, which also includes equal loading protein, Tubulin.

The other normalization procedure was the standard one which depends on the equal loading protein intensities. This optimization was applied after the first optimization was made. The intensity of each of the interested band values divided to values of the house-keeping protein intensity from the related samples, which is tubulin in these experiments.

2.4 Immunohistochemistry

Immunohistochemistry (IHC) is one of the methods for showing the correlation between morphology and specific antigen locations. This method is widely used in the diagnostic and research laboratories for different aims. For instance, IHC enables to diagnose a tumor type or determine the grade of it with using specific markers in diagnostic laboratories. Meanwhile, in the research field, IHC gives a chance to detect the location of specific proteins or other antigens in tissue sections to show cell death and repair.

This method includes three main parts, which are tissue fixation-preparation, sectioning, and staining.

Fixation can be performed three ways; air drying, snap freezing, and chemical fixation [111]. Selection of tissue preparation method depends on tissue type, the prevalence of experiment, and preferred sectioning method. Chemical fixation with alcohol, acetone, and formaldehyde is the most common type of fixation. Formaldehyde has more advantages to preserve morphological details. However, fixation is not enough alone to preserve morphological details. Thus, cryoprotection should be performed to preclude freezing artifacts. Cryoprotection can be made with serially diluted chemicals like sucrose or methanol to remove liquids in tissue. Embedding is the final step of the first part. Most frequently used embedding the tissues made with using paraffin or Optimal Cutting Temperature (OCT) compound.

Sectioning can be made with vibratome, microtome, or cryostat according to the thickness preference, sample preparation method, and tissue type. Vibratome or microtome allows taking a wide range of thickness of sections from paraffin-embedded tissues with harder to operate. On the other hand, cryostat allows taking thin

sections from frozen tissues with operating manually. Also, using cryostat is beneficial to small tissues rather than vibratome or microtome.

Staining methods show many differences. Mainly, the parts which include antigen retrieval, blocking, primary antibody incubation, secondary antibody incubation, and mounting. All of these process show alterations according to tissue thickness, type, and preferred antibody.

Protocols show differences according to the model organism, tissue, and antigen. Many different optimized protocols that were published before, are for the rodents or human tissues. However, finding an optimized protocol for zebrafish as a less commonly used model organism is more complicated. So, the new protocol was needed to develop for this research.

2.4.1 Optimization of the protocol

2.4.1.1 Tissue preparation:

In this step, fixation was made with paraformaldehyde. Overnight incubation is the suggested method in the product sheet. Afterward, initially, sections were processed without cryoprotection with sucrose. However, it caused deformation of the brain since the brains were frozen with liquid in the brain. So, sucrose steps were added. After the cryoprotection, brains were taken and embedded in O.C.T. product and directly put in -80 $^{\text{o}}$C without snap freezing because the orientation of the brain is crucial for sectioning part and making snap freezing caused orientation changes in the mold.

2.4.1.2 Sectioning

Sectioning was made with cryostat (Leica Biosystems, Germany, CM1850 UV). Cryostat method enables thinner sections as well as use of less antibody and the benefit of manual control in sectioning.

In the first trials, sections were taken at 10-micron thickness. However, it caused disruption of some markers and made it harder to design stereologically. 10-micron sections could not show appropriate visualization of GFAP. So, sections were taken as 20-micron of the whole brain.

Design of slides is based on selected stereology design. This research aimed to show key neuronal markers and one glial marker location in the whole brain. So, having one representative brain sample in one slide is beneficial for this aim. Thus, sections are located on slide separated in equal distance to each other, and to have at least one sections per brain area in one slide. Representative slide organization can be shown in the Figure 2.1. Thanks to this design, making staining for each antibody from each sample can be completed with staining only one slide. Slides were located in slide boxes and stored at -80 $^{\circ}$C until staining.

2.4.1.3 Staining

Staining part includes most changeable steps. Firstly, some of the antibodies need antigen retrieval step to bind the target protein epitope efficiency before starting staining. However, antigen retrieval has the potential to damage the tissue, especially in the case of frozen tissues. Therefore, each antibody which was used in this study firstly tried without antigen retrieval and used only when it was indispensable and cannot be compensated with the following step differences. Slides need to be thawed on ice until it comes to room temperature after they are taken from -80 $^{\circ}$C. Then, washing steps should be performed with 1x TBS-Triton or 1x PBS-Triton buffers before blocking. PBS buffer was observed to cause morphological distortion and more background. So, TBS was preferred over PBS as the washing buffer. TBS-Triton reduces surface tension while letting reagents to cover the whole sections easily. The volume of Triton in the buffer play role on penetration of the buffer to the tissue.

However, using a more than necessary amount of Triton cause tissue deformation and boost signal. 0.025% TritonX-100 was used in the final version of the protocol after the optimization.

Blocking buffer was prepared with using bovine serum albumin (BSA) rather than related serums of antibodies. It prevents possible nonspecific binding in the antibody incubation step. Primary and secondary antibodies in this study were not used before on the cryostat sections. Thus, optimization of antibodies were performed.

2.4.2 The optimized version of the Protocol

2.4.2.1 Tissue Preparation

2.4.2.1.1 Dissections

Dry weights and lengths of the fish were measured before decapitation. Heads were decapitated from the body with a scalpel blade after euthanasia. The head was placed as dorsal side in downward under the stereomicroscope. Gender determinations were made with opening peritoneal cavity and the existence of eggs or testis. After this step, 1 x PBS buffer (the recipe can be seen in the solutions part) added to cover the entire tissue to avoid possible damage during ablation of the brain. Other connective tissues were removed until reaching the skull and detecting the optic chiasm. Connectivity of optic chiasm between one of the eyes was cut off. Then, the eyes were removed and taken to another place. Cutting off the optic chiasm prevents pulling the brain to one side while taking the eyes. Removing them was revealed the skull. Skull was broken carefully, and the brain was checked from the ventral side. Then, it was extracted carefully and checked again for the existence of all structures, and the rest of the tissues were removed. After extracting the brain, all measured tissues were prepared to follow related steps to store the tissues other than the brain or fixation for brains. All other associated tissues which were eyes and bodies were put into 1.5 ml

eppendorf tubes separately, weighed quickly, and snap frozen immediately. Snap freezing made with using liquid nitrogen to avoid further degradation. Bodies and eyes were stored -80°C until the protein isolation.

2.4.2.2 Fixation Brain

Brains were placed carefully into the 2 ml eppendorf tubes, which already included 300µl fixation buffer (FB001, Invitrogen IC Fixation Buffer, Invitrogen, USA). Tubes were located in a rack in + 4 °C for overnight incubation for fixation.

2.4.2.3 Cryopreservation:

After the overnight incubation of brains, fixation buffer was removed with using fine tips and 1.5 ml 10% sucrose solution was added immediately to the brain. Sucrose solutions were always prepared the same day and stored at + 4 °C for cooling at least 1 hour before the fixation ends. Brains were incubated 2 hours in the 10% sucrose solution at + 4 °C. After, removing 10% sucrose solution, 1.5 ml 20% sucrose solution was added and stayed for 3 hours in incubation. 30% Sucrose solution was added after removing 20% sucrose solution and kept overnight incubation at + 4 °C which was the last step of cryopreservation. The times of incubation were decided according to sinking time of brains in solution.

2.4.2.4 Embedding brains

Disposable Base Molds 15x15x5mm (Electron Microscopy Sciences, PA, USA, #62534-15) were covered with Optimum Cutting Temperature (O.C.T.) compound (Tissue-Tek, Sakura, EU, #4583) which was taken from +4 °C until the half height of the base. Air bubbles were removed to eliminate possible artifacts and misdirection of the brain while freezing. Brain was put to the base and outside of the

mold was labeled in detail informing the direction of the brain for avoiding the mistakes in sectioning. The mold was covered with O.C.T. compound completely and placed in -80 °C with the help of a tray carefully. After frozen, molds were covered with labeled aluminum foil and stored at -80 °C until the sectioning.

2.4.2.4.1 Solutions

1. **PBS (10 X, 1 L)**

10 X PBS was prepared with using reagents in the Table 2.13. They were dissolved in 800 ml double distilled water. Then pH is adjusted to 7.4. After pH adjustment double distilled water was added up to 1 L and autoclaved.

Table 2. 13 Recipe of 10x PBS

Materials	Amount (for 1 L)
1.37 M NaCl	80 g
27 mM KCl	2 g
0.1 M $Na_2HPO_4.2H_2O$	15.2 g
15 mM KH_2PO_4	2 g

2. **10% sucrose solution**

500 mg sucrose (Sigma-Aldrich UK; catalog number S9378) was dissolved in 3ml 1 X PBS. Then 1 X PBS was added up to 5 ml.

3. **20% sucrose solution**

1 g sucrose was dissolved in 3ml 1 X PBS. Then 1 X PBS was added up to 5 ml.

4. **30% sucrose solution**

1.5 g sucrose was dissolved in 3ml 1 X PBS. Then 1 X PBS was added up to 5 ml.

2.4.2.5 Sectioning

Design of the sectioning was made under the guidance of the zebrafish brain anatomy atlas [95]. The aim of the design was to reach a representative whole brain in each slide from one brain. For this aim, 20 slides which have 9 sections in each of them were used for each subject. Representative slide design can be seen in Figure 2.1.
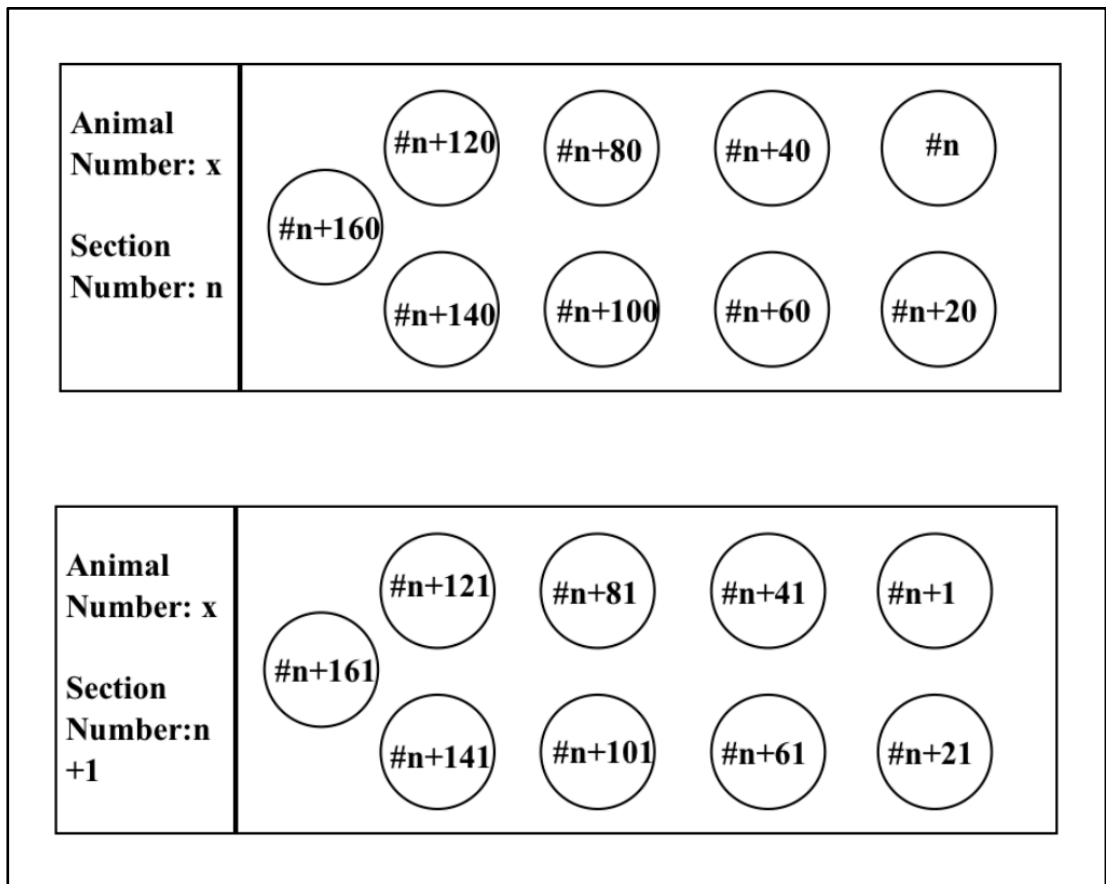
Figure 2.1 Representative image of slide design.

Sectioning was made using a cryostat (Leica Biosystems, Germany, #CM1850,). The temperature of the machine was fixed to -30 $^{\circ}$C and brains were located with molds in the machine for 30 minutes incubation to avoid the breakage of O.C.T. embedded tissue. After 30 minutes of incubation, the temperature of O.C.T. compound became sectile. Machine temperature was shifted to 25 $^{\circ}$C. One of the specimen plates was covered with two layers of O.C.T. compound. After each covering step, the thermal block was used to flatten the O.C.T. compound on the specimen plate. The O.C.T compound block in which the brain was embedded was removed from the mold and located on the parking station. Lateral parts of block were cut with using the blade for making it easy to handle and the frontal part was labeled. Specimen plate which is already covered was located on one of the quick freeze shelves. Adequate amount of O.C.T compound was added to attach the brain block on the specimen. The brain was attached perpendicularly, and the brain stem being closest to the specimen plate. The whole block covered with extra O.C.T compound until complete attachment was ensured, and the surface was flattened with using cold blade before O.C.T compound freeze. Specimen plate was placed and fixed in orientable specimen head, and angle of head was fixed as to be parallel to knife holder. Sectioning thickness was fixed to 20 μm, and started. Sections were collected according to the design of slides. Slides were located on the slide box and stored until staining in -80 $^{\circ}$C.

2.4.2.6 Staining

First, slides were taken from -80 $^{\circ}$C and placed on ice for 30 minutes. Then, antigen retrieval was performed, when necessary.

2.4.2.6.1 Antigen Retrieval

Distelled water was added up to the maximum level of Steamer (Tefal, Turkey, VC100115) and sterile tip box which filled up to half with sodium citrate buffer was located in the tier of the steamer. Then, the steamer was opened when 30 minutes on ice incubation was started. Slides were located in to the tip box. Antigen retrieval was performed for corresponding time of each antibody in this study for 30 minutes. After the end of the time, slide box was removed from steamer and waited 5 minutes in room temperature and about 10 minutes in +4 $^{\circ}$C until they reach room temperature.

2.4.2.6.1.1 Solution

1. **Sodium Citrate Buffer**

2.94 gram sodium Citrate (dihydrate) was dissolved in double distilled water to make a 10mM solution. Volume was completed to 1L after the pH was adjusted to 7.6 with 1 N HCl and then 0.5 ml of Tween-20 was added. This solution was stored at +4 $^{\circ}$C.

2.4.2.6.2 Washings and preparation for blocking

Slides were removed from sodium citrate buffer and dried gently. Glass staining dish (Fisher Science, USA, #08817) was filled up to slide level with Tris Buffered Saline with Tritonx100 (TBS-Triton), and slides were located in the staining dish vertically. Slides were washed for five times at room temperature with gentle agitation. Duration of washings were 5, 5, 5, 15, 15 minutes. After the washings, slides were dried, TBS-Triton which were around the sections were removed gently with tissue paper. Brain areas were drawn with using ImmEdge hydrophobic Barrier PAP pen (Vector Laboratories, USA, #101098-065).

2.4.2.6.2.1 Solution

1. **Tris Buffered Saline with Tritonx100:**

250 µl Triton x-100 (Sigma Aldrich, Germany, #T8787) was added 1L 1 x TBS and mixed well.

2.4.2.6.3 Blocking and Antibody Incubations

Slides were located in the Petri dishes and edges of the Petri dishes were covered with wet tissue papers to avoid sections from drying. Areas of brain sections were covered with blocking buffer and incubated one hour at room temperature. After the blocking, slides were dried gently, and were covered with corresponding primary antibodies.

For immunohistochemistry part, five different antibodies were used and each of them were diluted in blocking buffer. Anti-NeuN (Abcam, Cambridge, UK: ab177487, 1:5000 dilution), anti-HuC (Abcam, Cambridge, UK: ab78467, 1:100 dilution), anti-DCAMKL-1 (Abcam, Cambridge, UK: ab109029, 1:300 dilution), anti-GFP (Abcam, Cambridge, UK: ab6556, 1:1000 dilution) and anti-MAP-2 (Abcam, Cambridge, UK: ab32454, 1:1250 dilution) were primary antibodies in this study. Slides were transferred to the cold room for two days incubation. Every day, tissue paper was humidified which covered the Petri dishes. After two days incubation slides were taken from the cold room, and primary antibodies were removed from sections. Slides were washed for five times at room temperature with gentle agitation. Duration of washing steps were 5, 5, 5, 15, 15 minutes. After washing steps, slides were dried, and immediately fluorophore-conjugated secondary antibody (Cell Signaling Technology, Danvers, AM, USA: #4413, 1:1000 dilution) was poured on sections and incubated two hours at room temperature in dark. After the incubation 1x TBS washings were made with 5, 5, 5 minutes duration without agitation in the dark.

Table 2. 14 Antibody information for Immunohistochemistry experiments

Antibody Name	Specifications	Dilution	Antigen retrieval	Secondary antibody
NeuN	Mature neuron	1:5000	No	Anti-rabbit Alexa 555
HuC	Immature	1:100	Yes	Anti-rabbit Alexa 555
MAP-2	Mature	1:1250	Yes	Anti-rabbit Alexa 555
DCAMKL-1	Progenitor	1:300	Yes	Anti-rabbit Alexa 555
GFP	Glia	1:1000	No	Anti-rabbit Alexa 555

2.4.2.6.3.1 Solution

1. **Blocking buffer:**

0.5 g BSA was dissolved in 10 ml TBS-Triton.

2.4.2.6.4 Mounting

After the last washing step, slides were dried entirely and covered with mounting medium and carefully closed with a coverslip. In this part, removing all air bubbles was crucial for imaging well. The edges were stabilized with nail-polish. Covered slides were stored at +4 $^{\circ}$C.

2.4.2.6.5 Imaging

Imaging was made with the upright fluorescent microscopy. Zeiss-Axio vision and Zen Blue Edition software were used to image acqusition. All slides of the same antibody was measured with fixed parameters in software such as, contrast, binning, and exposure time with using 20x lens.

2.4.2.6.6 Counting and Density measurement

Counting and Density measurement were performed by using ImageJ software. For counting, point tool was used with selecting the options of add to overlay and label points. For intensity measurement of the positive signals of non-countable marker

which is GFP to mark GFAP, region of interest manager was used. Positive signals were matched with threshold marking and area fraction values of matched areas to whole area were used for analysis.

CHAPTER 3

RESULTS

3.1 Western Blot Results

Results in this section were obtained from protein band intensity of the whole brains. All data were obtained after the within gel and tubulin normalizations. Progenitor, immature, mature and glial markers were used in this chapter to show corresponding differences on age, gender, and their interactions. Before the two-way analysis of variance (ANOVA) was applied on data, normal distribution and homogeneity of variance of each data set was measured with the significance level set as 0.05. If the assumptions of normal distribution and homogeneity of variance were not violated, two-way ANOVA (as a parametric test) was applied to each data set.

3.1.1 Progenitor marker, DCAMKL-1

DCAMKL-1 is used according to the homology of doublecortin in mammalian vertebrates as a progenitor marker. Representative image of gel is shown in Figure 3.1.1. A two-way analysis of variance was conducted on the influence of two independent variables, which were age with two levels (young and old), and gender (female and male) on the normalized band intensity of DCAMKL-1. All effects were accepted as statistically significant, if they were at lower than the .05 significance level. The main effect of age yielded an F ratio $F_{(1,28)} = 3.519$, $p = 0.071$, indicating no significant difference between old and young. The main effect of gender was revealed $F_{(1,28)} = 0.513$, $p = 0.480$ as no significant difference, and Bonferroni test was applied to make multiple comparison between them. Multiple comparison shows that the expression level of DCAMKL-1 was significantly reduced in the old male group compared to young male group ($p = .048$).
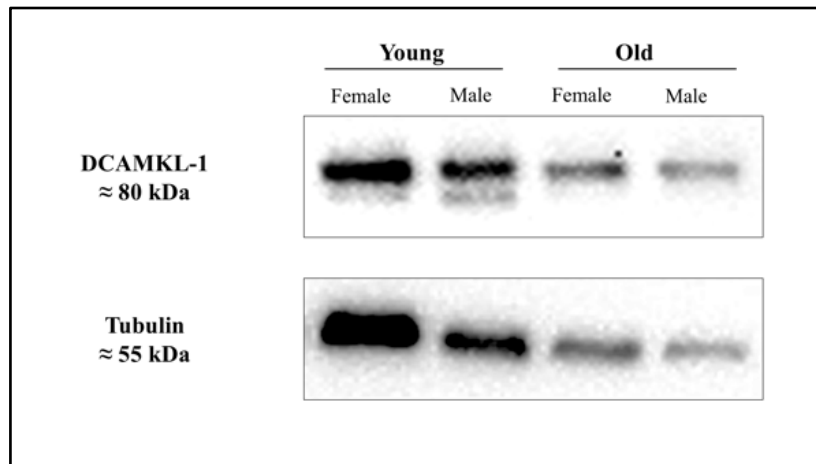
Figure 3.1 Representative gel image for DCAMKL-1 and each related groups were labelled above the bands.
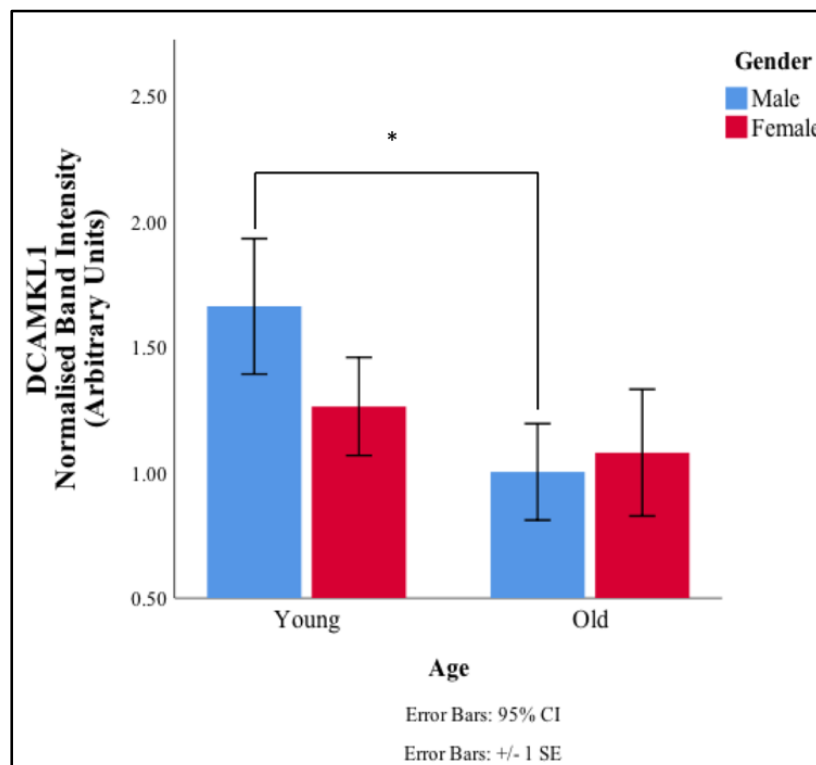
Figure 3.2 DCAMKL-1 expression across gender and age groups; Within gel and Tubulin normalized data. Error bars show +SE, * symbol $p<0.05$. The graph shows age has impacts on DCAMKL-1 expression level within male groups.

3.1.2 Immature Neuron Marker, HuC

HuC was used as immature early neuronal marker. Two-way ANOVA was applied to the HuC data set. The main effect of age F (1,28) = 5.587, p = 0.025, indicating statistically significant decline with aging, old group showed lower protein level rather than young group but no main effect of gender with two levels F (1,28) = 0.380, p= 0.542, was reported. On the other hand, interaction between age and gender results indicated that old males show statistically significant decline of HuC levels than young males, F (1,28) = 4.462, p = 0.044. Thus, immature neuron level is parallel with progenitor level.

Figure 3. 3 Representative gel image for HuC and each related groups were labelled above the bands.
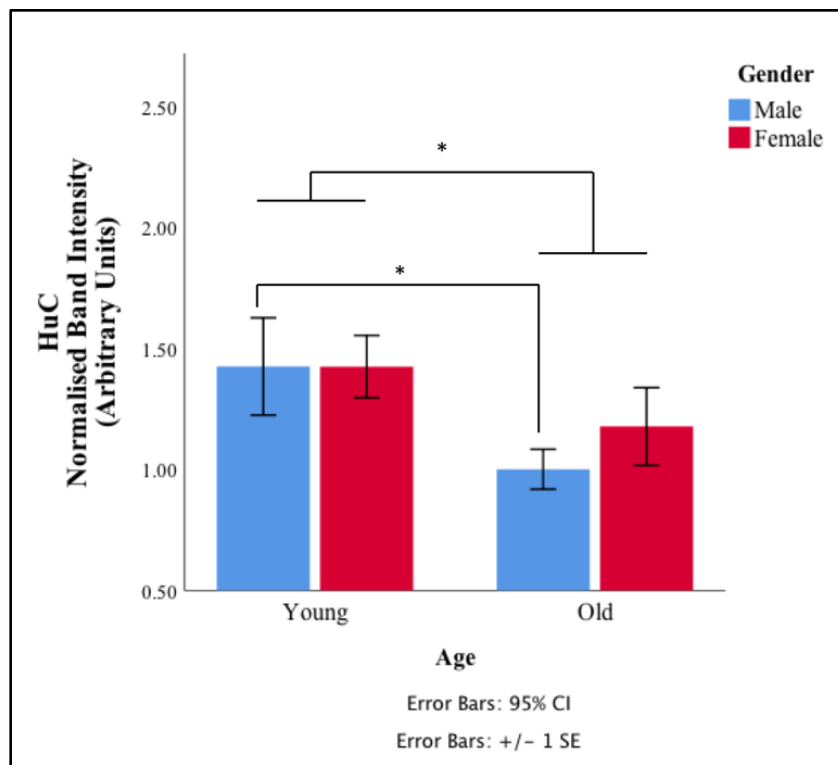
Figure 3.4 HuC expression across gender and age groups; Within gel and Tubulin normalized data. Error bars show +SE, * symbol p<0.05. The graph shows age has impacts on HuC expression level especially in male groups.

3.1.3 Mature Neuron Marker, NeuN

In Western Blot experiments NeuN was used to mark mature neurons. Neun is one of the most commonly used marker to detect mature neurons in all vertebrates with specification only to the post mitotic mature neurons. NeuN as a mature neuron marker shows general neuronal differences with aging and gender. Two-way ANOVA was used to measure statistical differences of NeuN level with aging, gender, and their interaction. The results of NeuN antibody shows no statistically significant change with age $F_{(1,28)} = 0.693$, gender $F_{(1,28)} = 0.623$ and their interaction $F_{(1,28)} = 0.615$.
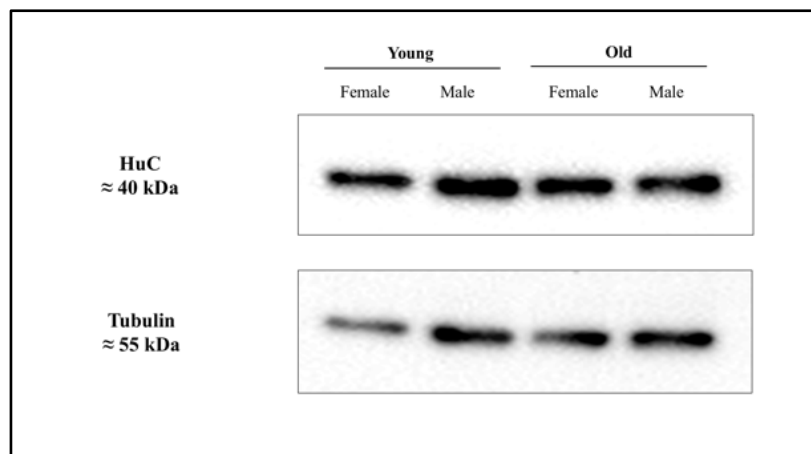
Figure 3.5 Representative gel image for NeuN and each related groups were labelled above the bands.
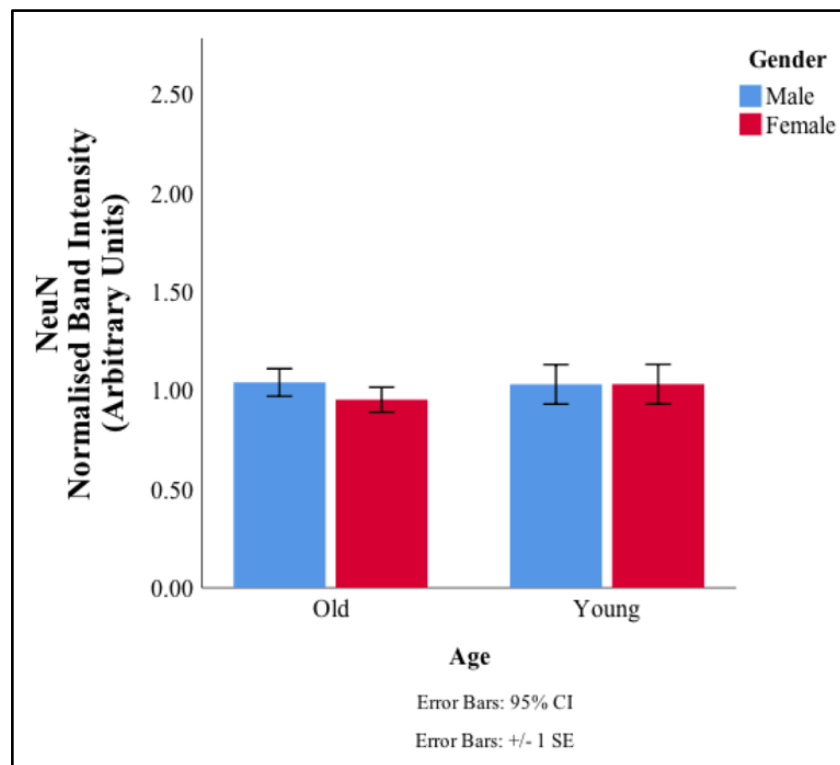
Figure 3.6 NeuN expression across gender and age groups; Within gel and Tubulin normalized data. Error bars show +SE.

3.1.4 Glial Marker, GFAP

GFAP was used to mark astrocytes in the whole brain lysates. Two-way ANOVA was performed on the GFAP data after the normality and homogeneity assumptions were checked. The main effect of age on GFAP yielded an $F(1,28) = 6.872$, $p = 0.014$, indicating significant differences between old and young. GFAP levels decreased significantly with aging. The main effect of gender yielded an $F(1,28) = 0.103$, $p = 0.750$, indicating no statistically significant differences between male and female.

Interaction of age and gender levels was referred that females in two age level which are young and old show statistically significant difference $F(1,28) = 6.346$, $p = 0.018$ whereas males show no statistically significant change on age levels $F(1,28) = 1.412$ and $p = 0.245$.
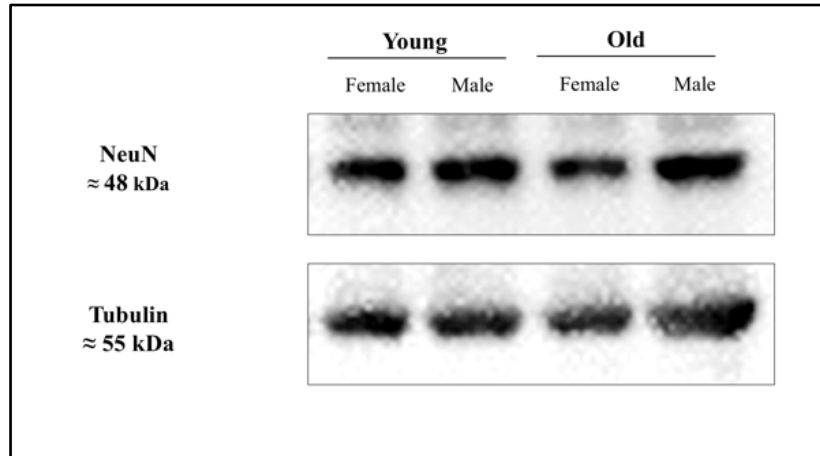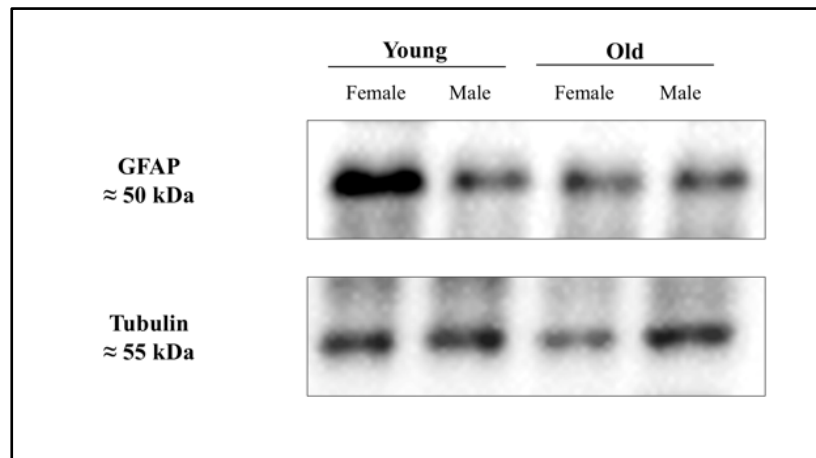

**Figure 3.7** Representative gel image for GFAP and each related groups were labelled above the bands.
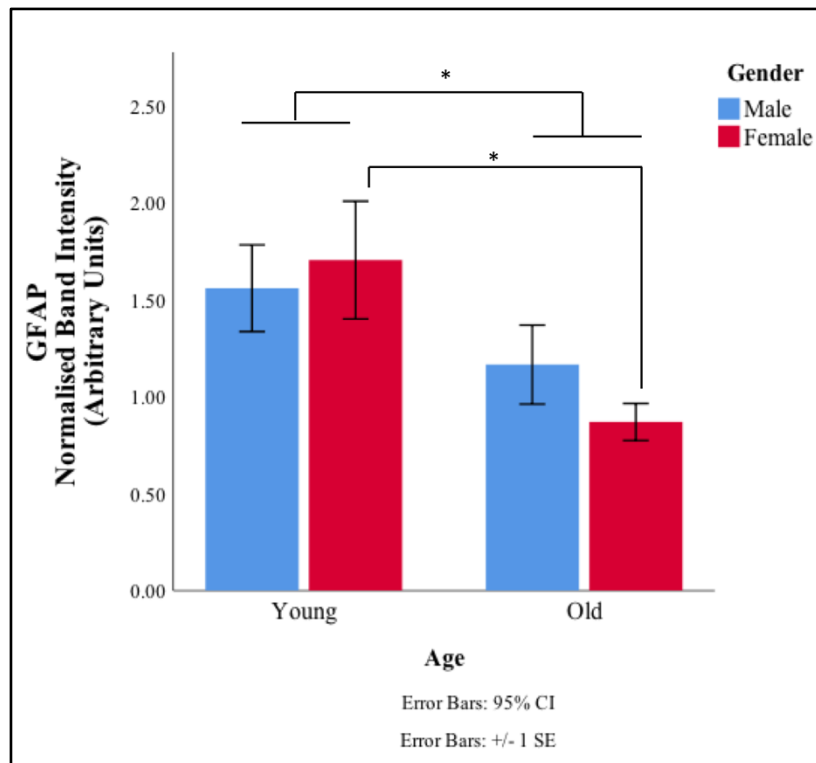
Figure 3.8 GFAP expression across gender and age groups; Within gel and Tubulin normalized data. Error bars show +SE, * symbol $p<0.05$. The graph shows age has impacts on HuC expression level especially in female groups.

3.2 Immunohistochemistry

In this part two different approaches were followed. First, related antibodies which are DCAMKL-1, HuC, NeuN, and MAP-2 were counted and GFP intensity was measured to show general neuronal marker number and astrocyte intensity changes in the whole brain sections. Then, two specific areas, which had the most proliferation in zebrafish brain, pallium, and optic tectum were selected for counting and intensity measurement. For this specific regions, images of four different antibody which are DCAMKL-1, HuC, MAP-2 and GFP were analyzed. All of the calculations were made by analyzing each related antibody by counting or by area fraction, then the sum of them was divided into their area. After each sections from one subject were calculated,

their average was taken for using data set. For counted antibodies, scale information were set and number of cell divided to micron square gained. All images were counted and areas were calculated with using ImageJ software.

3.2.1 Whole Brain Counting

In the first part, two young and two old subjects were used to get the general idea and their values were plotted. In this part because of the small sample size, statistical analysis were not applied into the data. Data were obtained from whole brain related cell numbers between two groups and were plotted with their calculated error bars.

3.2.1.1 DCAMKL-1 Counting

Whole brain countings of DCAMKL-1 as a progenitor marker did not show big differences between two age groups. Figure 3.9 shows corresponding chart for age related changes and representative image of DCAMKL-1 staining.
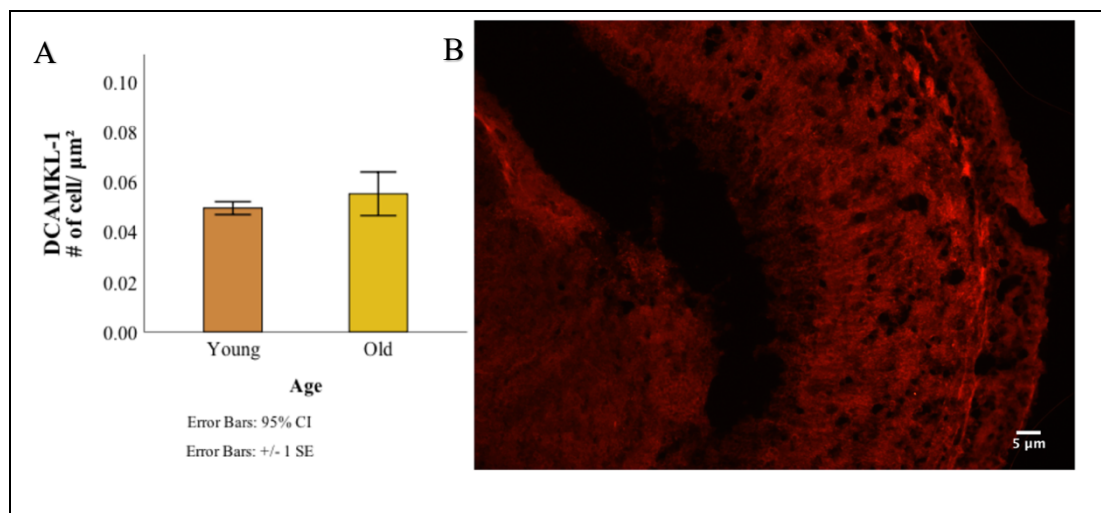
Figure 3.9 DCAMKL-1 does not change with aging. **A** Graph for number of DCAMKL-1 positive cells per micron square in whole brain and indicated that no significant change in the number of DCAMKL-1 positive cells. **B** shows representative image of an area from DCAMKL-1 stained section and image was taken with using 20 x lens.

3.2.1.2 HuC Counting

HuC as an early neuronal and immature neuron marker shows negligible change between two groups. Figure 3.10 shows graph of number of HuC positive cells and representative image of HuC staining.
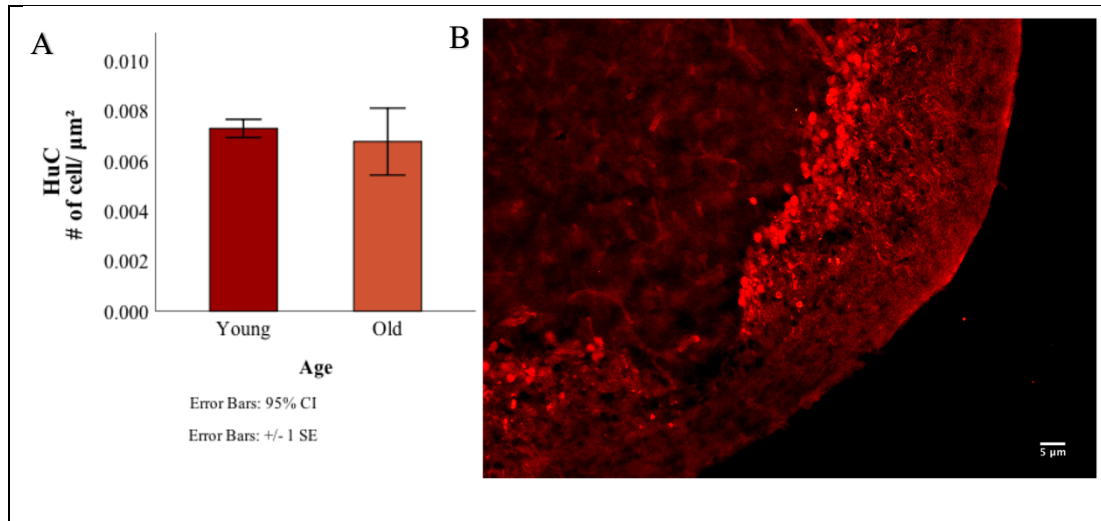
Figure 3.10 HuC positive cells in during aging. **A** age related changes in number of HuC positive cells per micron square in whole brain. Graph shows no significant changes between two age groups. **B** image was obtained from HuC antibody stained section, with using 20x lens.

3.2.1.3 NeuN Counting

NeuN is used as a mature neuron marker and it shows almost equal results between two age group. Figure 3.11 shows graph and representative image of NeuN antibody staining.
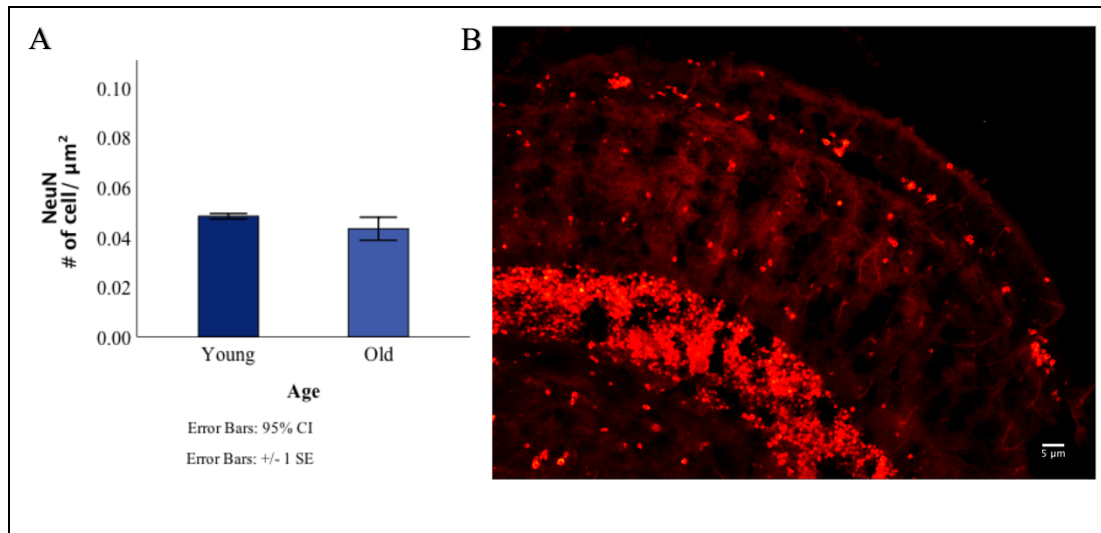
Figure 3.11 NeuN positive cells during aging. **A** Graph refers age related changes of whole brain NeuN positive cell numbers division to per micron square. **B** Image was taken from NeuN stained section, with using 20x lens.

3.2.1.4 MAP-2 Counting

MAP-2 was used as mature neuron marker but MAP-2 also has high expression in reactive astrocytes. Thus, this dual function makes MAP-2 as a bridge between mature neurons and astrocytes. Representative graph in Figure 3.12 indicates age related small increase of MAP-2 may explain the MAP-2 function as reactive astrocyte marker. Also, the increment of cell number is not seem as significant.
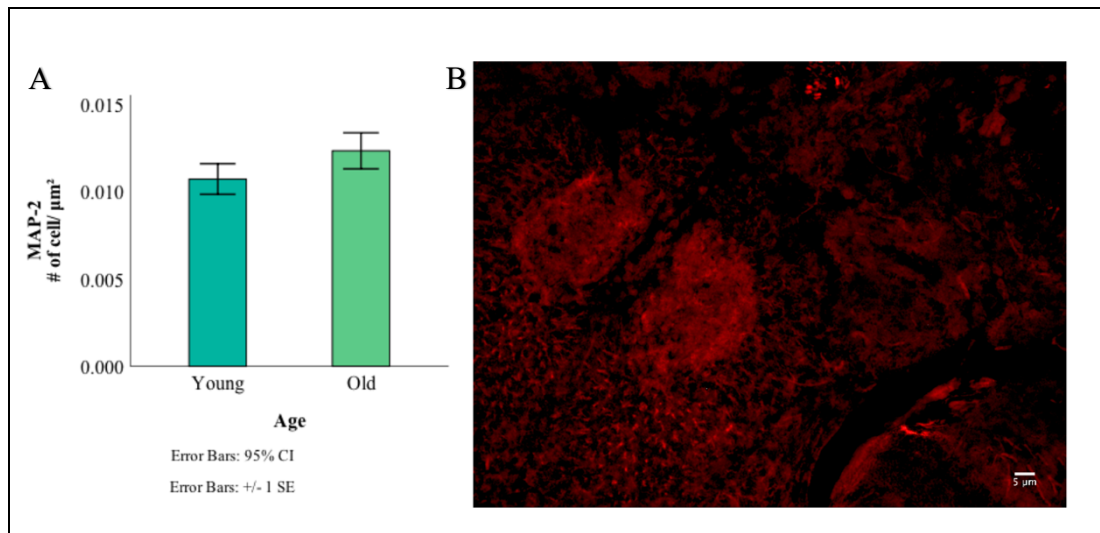
Figure 3.12 MAP-2 positive cells during aging. **A** Graph shows age related alteration of MAP-2 positive cell numbers per micron square and **B** image refers a part of MAP-2 stained section which was taken with 20x lens.

3.2.1.5 GFP counting

GFP antibody was used to enhance the signal of GFAP in transgenic line zebrafishes, glial fibrillary acidic protein (gfap): green fluorescent protein (GFP) which express GFP under the GFAP promoter. So, GFP was used as glial marker, especially astrocyte, in this study. Whole brain counting refers no significant difference between young and old groups. Since, age related small decline can be observable in astrocyte intensity as an opposite of MAP-2 as an reactive astrocyte number. Figure 3.13 shows related graph and representative image for GFP staining.
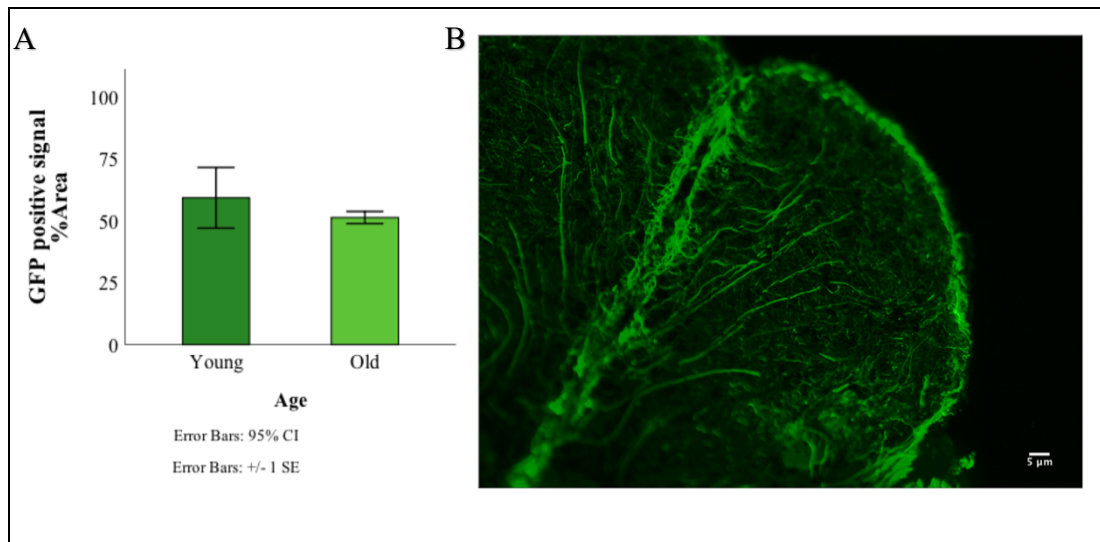
Figure 3.13 GFP tagged cells during aging. **A** Graph for whole brain area fraction of GFP positive signals change in aging and **B** representative image for GFP staining which was taken with 20x lens.

3.2.2 Pallium and Optic Tectum Counting

Pallium and optic tectum areas were selected by merging all images from each sections. Four different antibodies, which were DCAMKL-1, HuC, MAP-2 and GFP were counted from two specific regions. Eight subjects were included in that distribution as four young and four old. All areas were counted and divided to the related areas and then the mean was used. Normality and homogeneity of data sets were checked. If assumptions of parametric test were met, independent sample t-test was applied on data. If assumptions were not met, Mann Whitney U test was used to analyze data.

3.2.2.1 DCAMKL-1 counting

The progenitor marker counting indicated no statistical significant change between two age groups in pallium and optic tectum areas. After the data set was tested for homogeneity of variance and normal distribution, independent sample t-test was used to analyze DCAMKL-1 change during aging. There was no significant difference

in the counting for young (Mean= 0.092, Standard Deviation=0.024) and old (Mean=0.114, Standard Deviation=0.016) group; t(6)= (-1.512, p= 0.181). Related graph can be seen in Figure 3.14.
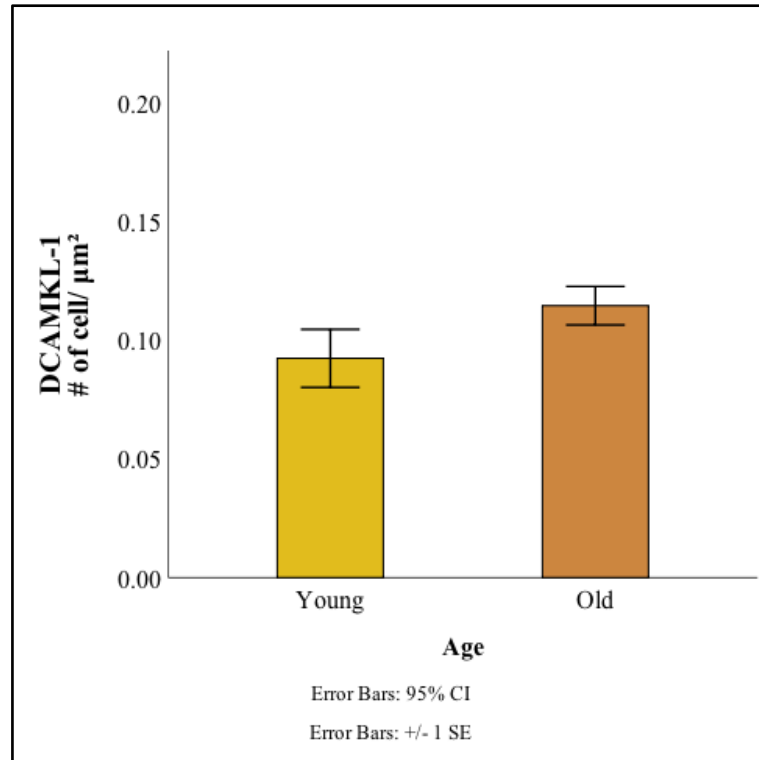
Figure 3.14 Age related changes in number of DCAMKL-1 positive cells per micron square in Pallium and Optic Tectum.

3.2.2.2 HuC Counting

To mark newborn neurons HuC was used in this part in the two proliferation zone, pallium and optic tectum. A Mann Whitney U test was conducted to evaluate the changes in the intensity of HuC positive cells between two age groups. The results of the test were indicated no statistically important difference between two groups, U= 5, z= -0.866, p = 0.486. Young group had an average rank of 3.75, while old group had an average rank of 5.25. Figure 3.15 represents related graph of the age related changes of HuC marker between two age groups.
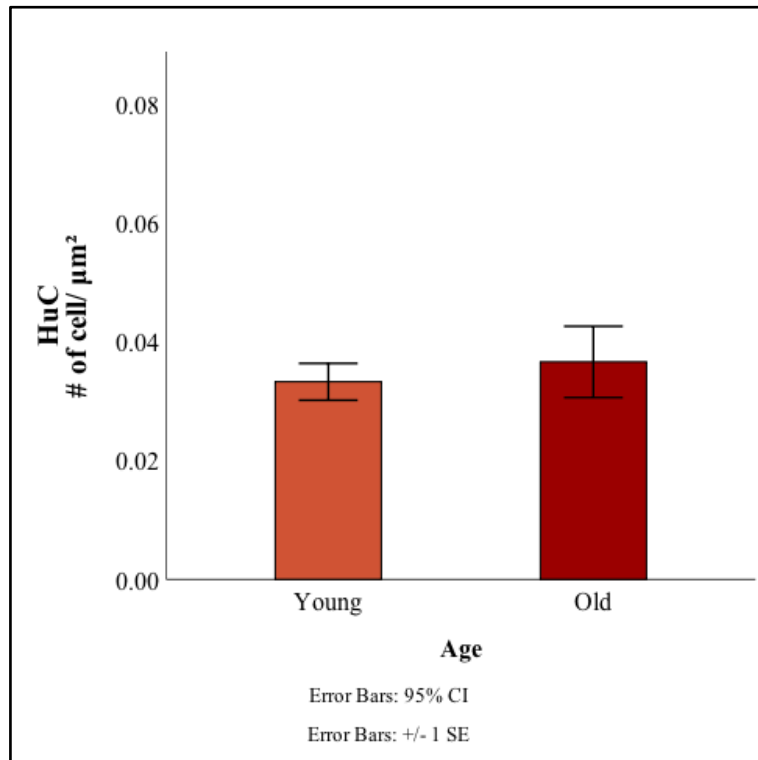
Figure 3.15 Age related changes in number of HuC positive cells per micron square in Pallium and Optic Tectum.

3.2.2.3 MAP-2 Counting

MAP-2 was used to mark mature neurons in the proliferation areas. A Mann Whitney U test was conducted to evaluate the changes in intensity of MAP-2 positive cells between two age groups. The results of the test indicated no statistically significant difference between young, which had a mean rank of 4.75, and old group, which had a mean rank of 4.25 , U= 7, z= -0.289, p = 0.886. The following graph in Figure 3.16 shows MAP-2 counting in pallium and optic tectum data distribution in young and old group.
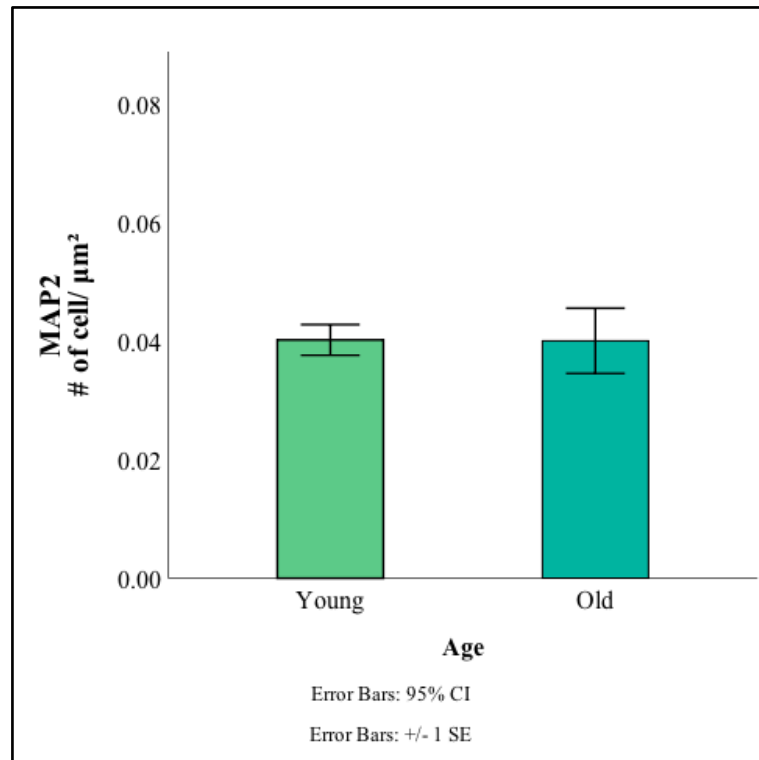
Figure 3.16 Age related changes in number of MAP-2 positive cells per micron square in Pallium and Optic Tectum.

3.2.2.4 GFP Intensity Measurement

GFP marked GFAP in this study, and measurement of GFP signal was done using ImageJ Region of Interest (ROI) measurement function and percentage of GFP positive signals in total area was used. There was no significant difference in the area fraction of GFP signal for young (Mean= 25.417, Standard Deviation=6.050) and old (Mean=25.948, Standard Deviation=3.047) group; $t(6)= (-0.157$ $p= 0.881)$. Related graph can be seen in Figure 3.17.
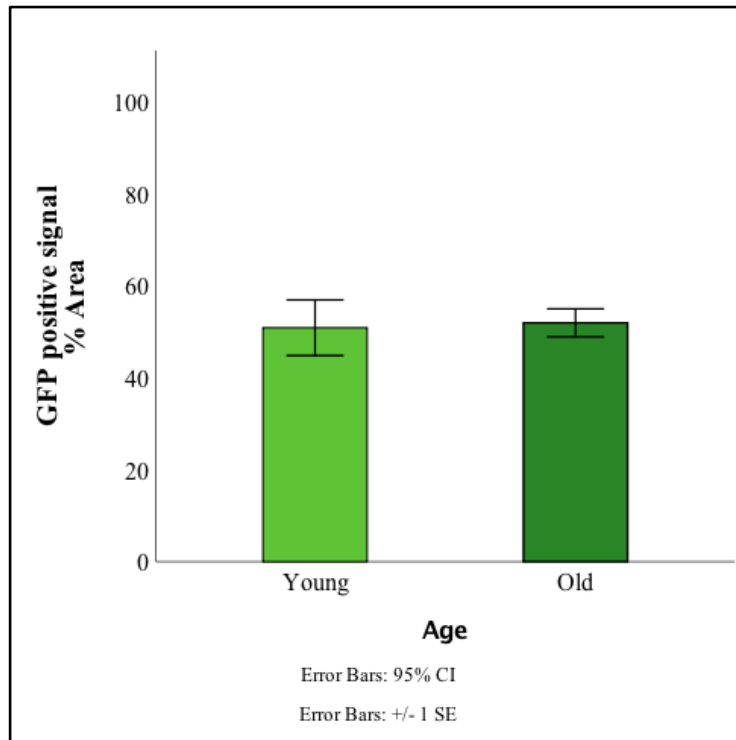
Figure 3.17 Age related changes in Pallium and Optic Tectum area fraction in GFP

positive cells per micron square.

CHAPTER 4

DISCUSSION

Aging is one of the most studied topics in neuroscience today. Understanding the underlying mechanisms of normal aging is crucial for dealing with age related disorders. Latest studies indicated no significant neuronal loss during normal aging process in mammalian brain. Also, we already know that neurogenesis continue in some specific proliferation zones during aging in mammalian brain. Zebrafish is a relatively new model organism in neuroscience research. Thus, we need to study on neuronal change in predicted proliferation areas and whole brain of zebrafish. For this aim two different ways can be followed; which are number of neuronal lineage markers and their corresponding protein levels.

The aim of this study was to show alterations in neuron number and protein levels of key neuronal markers by analyzing in two specific proliferation areas and whole brain during aging respectively. For this aim, two different techniques were performed. First, immunohistochemistry was used to analyze the specific areas where neuron numbers change. Then, whole brain neuronal and glial cell counting was performed as bridge of protein level differences in the whole brain. Pallium and optic tectum are too small for extracting proteins individually and it needs to be pool from multiple fish tissues. Also it has a potential to create confounding factors and missing data of individual differences. Thus, whole brain counting was performed to compare protein levels.

The results can be analyzed with two different ways. First, immunohistochemistry results show age related changes of neuronal and glial marker number in whole brain and two specific areas which are pallium and optic tectum.

Second, western-blot results indicated that age and gender have role in protein level differences in neuronal markers and one glial marker.

Cell count results did not indicate any statistically significant change in the markers used in neuronal proliferation areas. Statistically insignificant change of neural progenitor, immature and mature neuron markers are parallel with recent studies in human and the other vertebrates. However, the increase in GFAP levels with aging was indicated as a possible compensation of structural changes. Even in healthy aging, it directs neural inflammation.

Counting DCAMKL-1 as progenitor marker, in proliferation areas shows insignificant changes as mentioned before in the recent studies on hippocampal neurogenesis [112], [113]. Immature neuronal marker, HuC, showed parallelism with progenitor cell counting as expected. The other neuronal marker used was mature neuron marker, MAP-2, referred also insignificant alteration of numbers in proliferation zones. Thus, results indicated that aging did not cause decline in neuron number in zebrafish brain proliferation areas, as in mammalian brains, specifically in human. These results are a proof that zebrafish is an eligible model organism for brain aging research.

On the other hand, results of the astrocyte marker, GFAP, shows contradiction in some studies which refer to the increase in astrocyte number in the older ages compared with young subjects even in healthy aging in whole brain [114] and proliferation areas in mammalian's brain like hippocampus [115]. On the other hand, another study in mouse showed no change in hippocampus with respect to numbers of astrocytes [116]. Also, our results indicated statistically insignificant change between young and old zebrafish. This may explained as zebrafish feature of owing more

proliferation zone than mammals and life-long continuity of neurogenesis in multiple areas [117].

The aim of whole brain counting was to create preliminary data to compare protein level differences of the whole brain which were obtained from western blot results. Thus, whole brain counting results have limitations because of the small sample size and any statistical tests were not applied to them. Using whole brain lysate in western blot was preferred instead of using pooled pallium and optic tectum areas in order to be able to quantify biological differences. Results from whole brain counting did not indicate any big differences between two age groups.

Western blot experiments were performed with using bigger sample size and also sexual dimorphism were checked in addition to the age differences. Western blot results gave information about corresponding protein level differences in the whole brain. Protein regulation depends on more than one factor and these dependencies play a role on protein level differences. On the other hand, immunohistochemistry results show whether the cell is present or not without dependency of expression level in the certain time which brains were taken. Neurogenesis process taking different times [26] and expression level differences in this process has potential to reflect to changes of related protein levels in western blot analysis.

Protein level of progenitor and immature neuron markers indicated statistically significant decrease with aging in males while insignificant changes in females were observed. On the other hand, GFAP levels show significant decline in females whereas insignificant decrease in males' aging. Age related sexual dimorphism was demonstrated previously in gene expression levels [118] and synaptic proteins loss [119] in zebrafish.

Sexual dimorphism of DCAMKL-1 and HuC may explain with some different perspectives. One of them is that progenitor and immature neuron marker decrease in male aging may be the underlying mechanism of synaptic protein, Synaptophysin levels decrease in males during aging, which was mentioned in Karoğlu *et al* [119]. Relationship between Doublecortin and Synaptophysin in human brain was demonstrated before in Yuan and his colleagues study [120]. In this perspective, this study shows that the similar mechanisms play a role in aging between human and zebrafish.

Another possible factor of gender differences is that males have more brain atrophy than females during aging [121]. This atrophy may be related to sexual dimorphism of the progenitor and immature neuronal markers' protein levels decline in males significantly.

Western blot results of GFAP also show sexual dimorphism. However, the results indicated age related significant decline in females as an opposite of progenitor and immature neuronal markers. The compensatory role of astrocytes in neurogenesis may be a reason of that. Insignificant decline in males may be interpreted as compensatory system of significant decline in neuronal markers for males.

Only age-related changes were observed in HuC and GFAP as independent of gender impact. For age related decline in HuC as an parallel of DCAMKL-1 is expected feature and immature neurons decline also observed in old ages in mammalians brains with starting in adulthood [122].

GFAP protein level decline show opposite results with some previous studies which indicated astrocyte reactivity even in healthy aging [78], [114]; but reactive astrocytes at old ages were observed especially in neurodegenerative disease. Reactivity of astrocytes was started with immune response of neuronal changes and

then continuity of reactivity causes a toxic environment and neuronal loss in neurodegenerative diseases [123]. The age related decline of GFAP levels in our study may be explained with many different ways.

One possible reason of decline in GFAP can be explained with GFAP regulation in healthy aging. Research indicated that abnormal activities of GFAP in age related diseases but we did not know the gradual change in GFAP level during aging to death. We used the very old age animals in this study. Literature did not show the changes in very old ages. Autophagy mechanism may be activated in healthy centenarians, if the brain did not need to repair.

The other possibility of the decrease can be depended on characteristics of GFAP. GFAP is commonly used as astrocyte marker but also one commonly used progenitor marker in all vertebrates because of the high expression in radial glia. This multiple functions of GFAP may cause the decline with aging. In immunohistochemistry, detecting astrocytes according to their shapes are easy. However, in the protein level, GFAP may refer to multiple cell types and astrocytes in healthy tissues may not express GFAP [124],[81].

Mature neuron marker, NeuN, showed insignificant change during aging in protein levels. Recent studies indicated that human, mouse and many other vertebrates protect protein levels of mature neurons with aging.

Different results between cell numbers and protein levels shows that measuring protein levels cannot be a reliable way to comprehending time-consuming process of neurogenesis; because the changing expression level of related proteins may cause misleading results. Thus, future studies on neurogenesis should be focused on cell counting analysis.

CHAPTER 5

CONCLUSION AND FUTURE PROSPECTS

General aim of this study can be explained as investigating neuronal and glial level changes in different age and genders as well as their interactions. For this aim, first, age and gender related alterations was checked in the protein levels of neuronal and glial markers by using western blot technique. The results indicate that mature neuron levels which were measured with using NeuN antibody, does not change with age, gender, and their correlations which is parallel with recent studies on human and the other vertebrates. On the other hand, the other markers indicated some statistically significant changes in different levels. DCAMKL-1 as a progenitor marker showed statistically significant decline between young and old males, while no statistically significant change in age and gender levels separately. Changes of immature neuron level was checked with HuC. It showed a parallel feature of progenitor marker level changes in males. Additionally, HuC results indicate significant decline in young to old. GFAP as a glial marker, also, indicate age related significant decline especially in females.

Second, Immunohistochemistry experiments were made by focusing on two specific proliferation region in telencephalon and mesencephalon after preliminary experiments were performed on the whole brain. The second aim was detecting age related changes of neural progenitor, immature, mature and glial marker in these two regions. Results indicate that no statistically significant change during aging.

This study has some limitations. One of them is the sample size. Future experiments will need to be performed with increasing sample size, especially in immunohistochemistry parts. After increasing the sample size, gender differences should be checked in these groups as well. Another limitation is used marker number and their limited ability to cover all neurogenesis process. Some additional markers can be used in the following experiments to understand in detail. The other limitation can be dependent on age ranges in young and old groups. Additional age groups may be included in this study for understanding the gradual change of neural lineage markers during aging.

All in all, this study indicated that the neuronal numbers in two specific proliferation areas do not change during aging whereas protein levels of this specific markers show some changes in whole brain lysates; immature neuron and glial marker showed age related decline while progenitor, immature neuron and glial marker shows sexual dimorphism. Mature neuron number and protein level show insignificant changes between young and old groups as parallel with human brain. This study proves that zebrafish is a good gerontological model for studying adult neurogenesis.

Bibliography

[1]   C. López-Otín, M. A. Blasco, L. Partridge, M. Serrano, and G. Kroemer, "The hallmarks of aging.," *Cell*, vol. 153, no. 6, pp. 1194–217, 2013.

[2]   C. D. Mathers, G. A. Stevens, T. Boerma, R. A. White, and M. I. Tobias, "Causes of international increases in older age life expectancy," *Lancet*, vol. 385, no. 9967, pp. 540–548, 2015.

[3]   "Public Health and Aging : Trends in Aging — United States and Worldwide," *JAMA*, vol. 289, no. 11, pp. 1371–1373, 2003.

[4]   D. L. Murman, "The Impact of Age on Cognition," *Semin. Hear.*, vol. 36, no. 3, pp. 111–121, Aug. 2015.

[5]   A.-M. Kirova, R. B. Bays, and S. Lagalwar, "Working Memory and Executive Function Decline across Normal Aging, Mild Cognitive Impairment, and Alzheimer's Disease," *Biomed Res. Int.*, vol. 2015, 2015.

[6]   E. C. S. Künstler *et al.*, "Dual task effects on visual attention capacity in normal aging," *Front. Psychol.*, vol. 9, no. SEP, pp. 1–12, 2018.

[7]   C. Quigley and M. M. Muller, "Feature-Selective Attention in Healthy Old Age: A Selective Decline in Selective Attention?," *J. Neurosci.*, vol. 34, no. 7, pp. 2471–2476, 2014.

[8]   J. S. A. Carriere, J. A. Cheyne, G. J. F. Solman, and D. Smilek, "Age Trends for Failures of Sustained Attention," *Psychol. Aging*, vol. 25, no. 3, pp. 569–574, 2010.

[9]   R. C. Atkinson and R. M. Shiffrin, "Human memory: A proposed system and its control processes. In: Spence, KW.; Spence, JT., editors. The Psychology of Learning and Motivation: Advances in Research and Theory.," *New York:*

Academic Press, vol. 2. pp. 89–195, 1968.

[10] N. Cowan, "What are the differences between long-term, short-term, and working memory? Nelson," *NIH Public Access*, vol. 6123, no. 07, pp. 323–338, 2009.

[11] D. Friedman, D. Nessler, and R. Johnson, "Memory Encoding and Retrieval in the Aging Brain," *Clin. EEG Neurosci.*, vol. 38, no. 1, pp. 2–7, 2007.

[12] R. Cabeza *et al.*, "Age-related differences in neural activity during memory encoding and retrieval: a positron emission tomography study.," *J. Neurosci.*, vol. 17, no. 1, pp. 391–400, 1997.

[13] G. D. Laver, "Aging and Semantic Memory," no. Nilsson. 2017.

[14] J. D. Koen and A. P. Yonelinas, "The Effects of Healthy Aging, Amnestic Mild Cognitive Impairment, and Alzheimer's Disease on Recollection and Familiarity: A Meta-Analytic Review," *Neuropsychol. Rev.*, vol. 24, no. 3, pp. 332–354, 2014.

[15] N. Raz, P. Ghisletta, K. M. Rodrigue, K. M. Kennedy, and U. Lindenberger, "Trajectories of brain aging in middle-aged and older adults: Regional and individual differences Naftali," *Neuroimage*, vol. 51, no. 2, pp. 501–511, 2010.

[16] A. M. Fjell *et al.*, "High consistency of regional cortical thinning in aging across multiple samples," *Cereb. Cortex*, vol. 19, no. 9, pp. 2001–2012, 2009.

[17] E. R. Sowell, B. S. Peterson, P. M. Thompson, S. E. Welcome, A. L. Henkenius, and A. W. Toga, "Mapping cortical change across the human life span.," *Nat. Neurosci.*, vol. 6, no. 3, pp. 309–15, 2003.

[18] E. R. Lindemer, D. N. Greve, B. R. Fischl, J. C. Augustinack, and D. H. Salat, "Regional staging of white matter signal abnormalities in aging and

Alzheimer's disease," *NeuroImage Clin.*, vol. 14, pp. 156–165, 2017.

[19] F. Farokhian, C. Yang, I. Beheshti, H. Matsuda, and S. Wu, "Age-Related Gray and White Matter Changes in Normal Adult Brains," *Aging Dis.*, vol. 8, no. 6, p. 899, 2017.

[20] A. O'Shea, R. A. Cohen, E. C. Porges, N. R. Nissim, and A. J. Woods, "Cognitive aging and the hippocampus in older adults," *Front. Aging Neurosci.*, vol. 8, no. DEC, pp. 1–8, 2016.

[21] X. Li, Q. Li, X. Wang, D. Li, and S. Li, "Differential age-related changes in structural covariance networks of human anterior and posterior hippocampus," *Front. Physiol.*, vol. 9, no. MAY, pp. 1–9, 2018.

[22] A. M. Fjell *et al.*, "Critical ages in the life course of the adult brain: Nonlinear subcortical aging," *Neurobiol. Aging*, vol. 34, no. 10, pp. 2239–2247, 2013.

[23] C. S. von Bartheld, "Myths and truths about the cellular composition of the human brain: A review of influential concepts," *J. Chem. Neuroanat.*, vol. 93, no. August 2017, pp. 2–15, 2018.

[24] B. Alberts *et al.*, *Molecular Biology of the cell*, 6th ed. Garland Science, 2015.

[25] N. B. Metcalfe and P. Monaghan, "Growth versus lifespan : perspectives from evolutionary ecology," *Exp. Gerontol.*, vol. 38, pp. 935–940, 2003.

[26] C. Zhao, W. Deng, and F. H. Gage, "Mechanisms and Functional Implications of Adult Neurogenesis," *Cell*, vol. 132, pp. 645–660, 2008.

[27] C. Kizil, J. Kaslin, V. Kroehne, and M. Brand, "Adult Neurogenesis and Brain Regeneration in Zebrafish," *Dev. Neurobiol.*, vol. 72, pp. 429–461, 2012.

[28] P. S. Eriksson *et al.*, "Neurogenesis in the adult human hippocampus," *Nat. Med.*, 1998.

[29] J. L. Bizon, H. J. Lee, and M. Gallagher, "Neurogenesis in a rat model of age-

related cognitive decline," *Aging Cell*, pp. 227–234, 2004.

[30] E. Drapeau, W. Mayo, C. Aurousseau, M. Le Moal, P. Piazza, and D. N. Abrous, "Spatial memory performances of aged rats in the water maze predict levels of hippocampal neurogenesis," *PNAS*, vol. 100, no. 24, pp. 14385–14390, 2003.

[31] H. Liu and N. Song, "Molecular Mechanism of Adult Neurogenesis and its Association with Human Brain Diseases," *J. Cent. Nerv. Syst. Dis.*, vol. 8, pp. 5–11, 2016.

[32] D. A. Berg, L. Belnoue, H. Song, and A. Simon, "Neurotransmitter-mediated control of neurogenesis in the adult vertebrate brain," *Development*, vol. 140, pp. 2548–2561, 2013.

[33] H. A. Cameron, T. G. Hazel, and R. D. G. Mckay, "Regulation of Neurogenesis by Growth Factors and Neurotransmitters," *J. Neurobiol.*, vol. 36, pp. 287–306, 1998.

[34] C. Mirescu, J. D. Peters, L. Noiman, and E. Gould, "Sleep deprivation inhibits adult neurogenesis in the hippocampus by elevating glucocorticoids," vol. 103, no. 50, pp. 19170–19175, 2006.

[35] H. Van Praag, T. Shubert, C. Zhao, and F. H. Gage, "Exercise Enhances Learning and Hippocampal Neurogenesis in Aged Mice," *J. Neurosci.*, vol. 25, no. 38, pp. 8680–8685, 2005.

[36] R. M. Seaberg and D. Van Der Kooy, "Stem and progenitor cells : the premature desertion of rigorous definitions," *Trends Neurosci.*, vol. 26, no. 3, pp. 125–131, 2003.

[37] J. M. Hébert and J. Vijg, "Cell Replacement to Reverse Brain Aging: Challenges, Pitfalls, and Opportunities," *Trends Neurosci.*, vol. 41, no. 5, pp.

267–279, 2018.

[38]   J. P. Brown, B. Couillard-despre, C. M. Cooper-kuhn, J. Winkler, L. Aigner, and H. G. Kuhn, "Transient Expression of Doublecortin during Adult Neurogenesis," *J. Comp. Neurol.*, vol. 467, pp. 1–10, 2003.

[39]   T. A. S. Deuel, J. S. Liu, J. C. Corbo, S. Yoo, L. B. Rorke-adams, and C. A. Walsh, "Genetic Interactions between Doublecortin and Doublecortin-like Kinase in Neuronal Migration and Axon Outgrowth," *Neuron*, vol. 49, pp. 41–53, 2006.

[40]   P. T. Lin, J. G. Gleeson, J. C. Corbo, L. Flanagan, and C. A. Walsh, "DCAMKL1 Encodes a Protein Kinase with Homology to Doublecortin that Regulates Microtubule Polymerization," *J. Neurosci.*, vol. 20, no. 24, pp. 9152–9161, 2000.

[41]   H. A. Burgess, S. Martinez, and O. Reiner, "KIAA0369, Doublecortin-Like Kinase, Is Expressed During Brain Development Harold," *J. Neurosci. Res.*, vol. 575, pp. 567–575, 1999.

[42]   Y. Omori *et al.*, "Expression and chromosomal localization of KIAA0369 , a putative kinase structurally related to Doublecortin," *J. Hum. Genet.*, vol. 43, pp. 169–177, 1998.

[43]   S. Shimomura, T. Nagamine, T. Nimura, N. Sueyoshi, Y. Shigeri, and I. Kameshita, "Expression, characterization, and gene knockdown of zebrafish doublecortin-like protein kinase," *Arch. Biochem. Biophys.*, vol. 463, pp. 218–230, 2007.

[44]   F. Jiménez and J. A. Campos-ortega, "Genes in subdivision IB of the Drosophila melanogaster X-chromosome and their influence on neural development," *J. Neurogenet.*, vol. 4, pp. 179–200, 1987.

[45] H. Park *et al.*, "Structural comparison of zebrafish Elav / Hu and their differential expressions during neurogenesis," *Neurosci. Lett.*, vol. 279, pp. 81–84, 2000.

[46] H. Zhu, R. A. Hasman, V. A. Barron, G. Luo, and H. Lou, "A Nuclear Function of Hu Proteins as Neuron-specific Alternative RNA Processing Regulators," *Mol. Biol. Cell*, vol. 17, pp. 5105–5114, 2006.

[47] R. J. Mullen, C. R. Buck, and A. M. Smith, "NeuN , a neuronal specific nuclear protein in vertebrates," *Development*, vol. 116, pp. 201–211, 1992.

[48] J. R. Cannon and J. T. Greenamyre, "NeuN is not a reliable marker of dopamine neurons in rat substantia nigra," *Neurosci. Lett.*, vol. 464, pp. 14–17, 2009.

[49] S. S. Kumar and P. S. Buckmaster, "Neuron-specific nuclear antigen NeuN is not detectable in gerbil subtantia nigra pars reticulata," *Brain Res.*, vol. 1142, pp. 54–60, 2007.

[50] V. V. Gusel'nikova and D. E. Korzhevskiy, "NeuN As a Neuronal Nuclear Antigen and Neuron Differentiation Marker," *Acta Naturae*, vol. 7, no. 2(25), pp. 42–47, 2015.

[51] N. Hirokawa, T. Funakoshi, R. Sato-Harada, and Y. Kanai, "Selective stabilization of tau in axons and microtubule-associated protein 2C in cell bodies and dendrites contributes to polarized localization of cytoskeletal proteins in mature neurons," *J. Cell Biol.*, vol. 132, no. 4, pp. 667–679, 1996.

[52] R. W. L. Lim and S. Halpain, "Regulated association of microtubule-associated protein 2 (MAP2) with Src and Grb2: Evidence for MAP2 as a scaffolding protein," *J. Biol. Chem.*, vol. 275, no. 27, pp. 20578–20587, 2000.

[53] N. Chauhan and G. Siegel, "Age-dependent organotypic expression of

microtubule-associated proteins (MAP1, MAP2, and MAP5) in rat brain,"
Neurochem. Res., vol. 22, no. 6, pp. 713–719, 1997.

[54]   C. Sánchez, J. Díaz-Nido, and J. Avila, "Phosphorylation of microtubule-associated protein 2 (MAP2) and its relevance for the regulation of the neuronal cytoskeleton function.," *Prog. Neurobiol.*, vol. 61, pp. 133–68, 2000.

[55]   C. S. von Bartheld, J. Bahney, and S. Herculano-Houzel, "The search for true numbers of neurons and glial cells in the human brain: A review of 150 years of cell counting," *J. Comp. Neurol.*, vol. 524, no. 18, pp. 3865–3895, 2016.

[56]   B. Stevens *et al.*, "The Classical Complement Cascade Mediates CNS Synapse Elimination," *Cell*, vol. 131, no. 6, pp. 1164–1178, 2007.

[57]   J. P. Schwartz, "Microglia Function in CNS: Development and Plasticity," *Cold Spring Harb. Perspect. Biol.*, pp. 877–882, 2015.

[58]   A. Citri and R. C. Malenka, "Synaptic plasticity: Multiple forms, functions, and mechanisms," *Neuropsychopharmacology*, vol. 33, no. 1, pp. 18–41, 2008.

[59]   D. S. Davies, J. Ma, T. Jegathees, and C. Goldsbury, "Microglia show altered morphology and reduced arborization in human brain during aging and Alzheimer's disease," *Brain Pathol.*, vol. 27, no. 6, pp. 795–808, 2017.

[60]   B. Spittau, "Aging microglia-phenotypes, functions and implications for age-related neurodegenerative diseases," *Front. Aging Neurosci.*, vol. 9, no. JUN, pp. 1–9, 2017.

[61]   O. Butovsky and H. L. Weiner, "Microglial signatures and their role in health and disease," *Nat. Rev. Neurosci.*, vol. 19, no. 10, pp. 622–635, 2018.

[62]   N. Baumann and D. Pham-Dinh, "Biology of Oligodendrocyte and Myelin in the Mammalian Central Nervous System," *Physiol. Rev.*, vol. 81, no. 2, pp.

871–927, 2001.

[63]   J. D. Hinman, A. Peters, H. Cabral, D. L. Rosene, W. Hollander, and M. N. Rasband, "Age-Related Molecular Reorganization at the Node of Ranvier," *J. Comp. Neurol.*, vol. 362, no. May 2005, pp. 351–362, 2006.

[64]   H. Liu, Y. Yang, Y. Xia, W. Zhu, R. K. Leak, and Z. Wei, "Aging of cerebral white matter," *Ageing Res. Rev.*, vol. 34, pp. 64–76, 2017.

[65]   M. Simons and K. Nave, "Oligodendrocytes : Myelination and Axonal Support," *Cold Spring Harb Perspect Biol*, pp. 1–16, 2016.

[66]   Y. Lee *et al.*, "Oligodendroglia metabolically support axons and contribute to neurodegeneration," *Nature*, vol. 487, no. 7408, pp. 443–448, 2012.

[67]   N. Salvadores, M. Sanhueza, P. Manque, F. A. Court, and F. A. Court, "Axonal Degeneration during Aging and Its Functional Role in Neurodegenerative Disorders," *Front. Neurosci.*, vol. 11, no. September, 2017.

[68]   S. Herculano-houzel, "The Glia / Neuron Ratio : How it Varies Uniformly Across Brain Structures and Species and What that Means for Brain Physiology and Evolution," *Glia*, vol. 62, no. 9, pp. 1377–1391, 2014.

[69]   D. Attwell, A. M. Buchan, S. Charpak, M. Lauritzen, B. A. Macvicar, and E. A. Newman, "Glial and neuronal control of brain blood flow," *Nature*, vol. 468, pp. 232–243, 2010.

[70]   X. T. Sotelo-hitschfeld *et al.*, "Channel-Mediated Lactate Release by K+ - Stimulated Astrocytes," *J. Neurosci.*, vol. 35, no. 10, pp. 4168–4178, 2015.

[71]   K. H. Lauritzen *et al.*, "Lactate Receptor Sites Link Neurotransmission , Neurovascular Coupling , and Brain Energy Metabolism," *Cereb. Cortex*, vol. 24, no. October, pp. 2784–2795, 2014.

[72] Y. Ota, A. T. Zanetti, and R. M. Hallock, "The Role of Astrocytes in the Regulation of Synaptic Plasticity and Memory Formation," *Neural Plast.*, vol. 2013, 2013.

[73] M. Simard and M. Nedergaard, "The Neurobiology of Glia in the Contex of Water and Ion Homeostasis," *Neuroscience*, vol. 129, pp. 877–896, 2004.

[74] J. Woo *et al.*, "Astrocytic water channel aquaporin-4 modulates brain plasticity in both mice and humans : a potential gliogenetic mechanism underlying language-associated learning," *Mol. Psyhiatry*, vol. 23, pp. 1021–1030, 2018.

[75] S. Nielsen, E. A. Nagelhus, M. Amiry-moghaddam, C. Bourque, P. Agre, and O. P. Ottersen, "Specialized Membrane Domains for Water Transport in Glial Cells : High-Resolution Immunogold Cytochemistry of Aquaporin-4 in Rat Brain," *J. Neurosci.*, vol. 17, no. 1, pp. 171–180, 1997.

[76] E. M. Ullian, S. K. Sapperstein, K. S. Christopherson, and B. A. Barres, "Control of Synapse Number by Glia," *Science (80-.).*, vol. 291, no. January, pp. 657–662, 2001.

[77] W. Chung *et al.*, "Astrocytes mediate synapse elimination through MEGF10 and MERTK pathways," *Nature*, vol. 504, no. 7480, pp. 394–400, 2013.

[78] S. A. Liddelow *et al.*, "Neurotoxic reactive astrocytes are induced by activated microglia," *Nat. Publ. Gr.*, vol. 541, no. 7638, pp. 481–487, 2017.

[79] Lawrence F. Eng, Roopa S. Ghirnikar, and Yuen L. Lee, "Glial Fibrillary Acidic Protein: GFAP-Thirty-One Years (1969–2000)," *Neurochem. Res.*, vol. 25, no. 9/10, pp. 1439–1451, 2000.

[80] E. M. Hol *et al.*, "Neuronal expression of GFAP in patients with Alzheimer pathology and identification of novel GFAP splice forms," *Mol. Psychiatry*,

vol. 8, no. 9, pp. 786–796, 2003.

[81]   M. V Sofroniew and H. V Vinters, "Astrocytes: biology and pathology.," *Acta Neuropathol.*, vol. 119, no. 1, pp. 7–35, 2010.

[82]   N. Daschil and C. Humpel, "Green-fluorescent protein+ astrocytes attach to beta-amyloid plaques in an Alzheimer mouse model and are sensitive for clasmatodendrosis," *Front. Aging Neurosci.*, vol. 8, no. APR, pp. 1–6, 2016.

[83]   E. M. Hol and M. Pekny, "Glial fibrillary acidic protein (GFAP) and the astrocyte intermediate filament system in diseases of the central nervous system," *Curr. Opin. Cell Biol.*, vol. 32, pp. 121–130, 2015.

[84]   X. Chen, D. Gays, and M. M. Santoro, "GFAP Transgenic zebrafish," *Methods Mol. Biol.*, vol. 1464, pp. 107–114, 2016.

[85]   C. Nolte *et al.*, "GFAP promoter-controlled EGFP-expressing transgenic mice: A tool to visualize astrocytes and astrogliosis in living brain tissue," *Glia*, vol. 33, no. 1, pp. 72–86, 2001.

[86]   G. Kempermann, S. Jessberger, B. Steiner, and G. Kronenberg, "Milestones of neuronal development in the adult hippocampus," *Trends Neurosci.*, vol. 27, no. 8, pp. 447–452, 2004.

[87]   A. D. R. Garcia, N. B. Doan, T. Imura, T. G. Bush, and M. V. Sofroniew, "GFAP-expressing progenitors are the principal source of constitutive neurogenesis in adult mouse forebrain," *Nat. Neurosci.*, vol. 7, no. 11, pp. 1233–1241, 2004.

[88]   D. G. Amen, M. Trujillo, D. Keator, D. V Taylor, and K. Willeumier, "Gender-Based Cerebral Perfusion Differences in 46 , 034 Functional Neuroimaging Scans," *J. Alzheimer's Dis.*, vol. 60, pp. 605–614, 2017.

[89]   J. M. Goldstein, L. J. Seidman, N. J. Horton, N. Makris, D. N. Kennedy, and

V. S. Caviness, "Normal Sexual Dimorphism of the Adult Human Brain Assessed by In Vivo Magnetic Resonance Imaging," *Cereb. Cortex*, vol. 11, no. 6, pp. 490–497, 2001.

[90] R. C. Gur *et al.*, "Sex differences in brain gray and white matter in healthy young adults : Correlations with cognitive performance Sex Differences in Brain Gray and White Matter in Healthy Young Adults : Correlations with Cognitive Performance," *J. Neurosci.*, vol. 19, no. 10, pp. 4065–4072, 1999.

[91] E. Gould, A. J. Reeves, M. Fallah, P. Tanapat, C. G. Gross, and E. Fuchs, "Hippocampal neurogenesis in adult Old World primates," *Proc. Natl. Acad. Sci. USA*, vol. 96, no. April, pp. 5263–5267, 1999.

[92] R. Mahmoud, S. R. Wainwright, and L. A. M. Galea, "Sex hormones and adult hippocampal neurogenesis : Regulation , implications , and potential mechanisms," *Front. Neuroendocrinol.*, vol. 41, pp. 129–152, 2016.

[93] K. Howe *et al.*, "The zebrafish reference genome sequence and its relationship to the human genome," *Nature*, vol. 496, no. 7446, pp. 498–503, 2013.

[94] G. J. Lieschke and P. D. Currie, "Animal models of human disease: Zebrafish swim into view," *Nat. Rev. Genet.*, vol. 8, no. 5, pp. 353–367, 2007.

[95] M. F. Wullimann *et al.*, *Neuroanatomy of the Zebrafish Brain Deutsche Bibliothek Cataloging-in-Publication Data Neuroanatomy of the zebrafish brain: a topological atlas*. 1996.

[96] D. T. Mueller and M. Wullimann, *Atlas of Early Zebrafish Brain Development: A Tool for Molecular Neurogenetics*. 2015.

[97] J. Ganz, J. Kaslin, D. Freudenreich, A. Machate, M. Geffarth, and M. Brand, "Subdivisions of the adult zebrafish subpallium by molecular marker analysis," *J. Comp. Neurol.*, vol. 520, no. 3, pp. 633–655, 2012.

[98] J. Ganz *et al.*, "Subdivisions of the adult zebrafish pallium based on molecular marker analysis," *F1000Research*, vol. 3, no. 3, p. 308, 2015.

[99] R. Vargas, H. Thorsteinsson, and K. A. E. Karlsson, "Spontaneous neural activity of the anterodorsal lobe and entopeduncular nucleus in adult zebrafish: A putative homologue of hippocampal sharp waves," *Behav. Brain Res.*, vol. 229, no. 1, pp. 10–20, 2012.

[100] R. K. Cheng, S. J. Jesuthasan, and T. B. Penney, "Zebrafish forebrain and temporal conditioning," *Philos. Trans. R. Soc. B Biol. Sci.*, vol. 369, no. 1637, 2014.

[101] Y. Ito, H. Tanaka, H. Okamoto, and T. Ohshima, "Characterization of neural stem cells and their progeny in the adult zebrafish optic tectum," *Dev. Biol.*, vol. 342, no. 1, pp. 26–38, 2010.

[102] K. Hinsch and G. K. H. Zupanc, "Generation and long-term persistence of new neurons in the adult zebrafish brain: A quantitative analysis," *Neuroscience*, vol. 146, no. 2, pp. 679–696, 2007.

[103] J. Boulanger-Weill and G. Sumbre, "Functional Integration of Newborn Neurons in the Zebrafish Optic Tectum," *Front. Cell Dev. Biol.*, vol. 7, no. April, pp. 1–8, 2019.

[104] G. S. Gerhard *et al.*, "Life spans and senescent phenotypes in two strains of Zebrafish (Danio rerio)," *Exp. Gerontol.*, vol. 37, no. 8–9, pp. 1055–1068, 2002.

[105] M. M. Adams and H. Kafaligonul, "Zebrafish—A Model Organism for Studying the Neurobiological Mechanisms Underlying Cognitive Brain Aging and Use of Potential Interventions," *Front. Cell Dev. Biol.*, vol. 6, no. November, pp. 1–5, 2018.

[106] A. D. Collier, A. V. Kalueff, and D. J. Echevarria, *The rights and wrongs of zebrafish: Behavioral phenotyping of zebrafish*. 2017.

[107] L. Yu, V. Tucci, S. Kishi, and I. V. Zhdanova, "Cognitive aging in zebrafish," *PLoS One*, vol. 1, no. 1, 2006.

[108] T. Ruhl *et al.*, "Oxidation and Cognitive Impairment in the Aging Zebrafish," *Gerontology*, vol. 62, no. 1, pp. 47–57, 2015.

[109] K. Edelmann *et al.*, "Increased radial glia quiescence, decreased reactivation upon injury and unaltered neuroblast behavior underlie decreased neurogenesis in the aging zebrafish telencephalon," *J. Comp. Neurol.*, vol. 521, no. 13, pp. 3099–3115, 2013.

[110] A. Arslan-Ergul, B. Erbaba, E. T. Karoglu, D. O. Halim, and M. M. Adams, "Short-term dietary restriction in old zebrafish changes cell senescence mechanisms," *Neuroscience*, vol. 334, pp. 64–75, Oct. 2016.

[111] I. B. Buchwalow, *Immuno-histochemistry basic and methods*. 2010.

[112] M. Boldrini *et al.*, "Human Hippocampal Neurogenesis Persists throughout Aging," *Cell Stem Cell*, vol. 22, no. 4, pp. 589-599.e5, 2018.

[113] B. Hattiangady and A. K. Shetty, "Aging does not alter the number or phenotype of putative stem/progenitor cells in the neurogenic region of the hippocampus," *Neurobiol. Aging*, vol. 29, no. 1, pp. 129–147, 2008.

[114] L. E. Clarke, S. A. Liddelow, C. Chakraborty, A. E. Münch, M. Heiman, and B. A. Barres, "Normal aging induces A1-like astrocyte reactivity," *Proc. Natl. Acad. Sci.*, vol. 115, no. 8, pp. E1896–E1905, 2018.

[115] J. J. Rodríguez, C. Y. Yeh, S. Terzieva, M. Olabarria, M. Kulijewicz-Nawrot, and A. Verkhratsky, "Complex and region-specific changes in astroglial markers in the aging brain," *Neurobiol. Aging*, vol. 35, no. 1, pp. 15–23, 2014.

[116] S. Jinno, "Regional and laminar differences in antigen profiles and spatial distributions of astrocytes in the mouse hippocampus, with reference to aging," *Neuroscience*, vol. 180, pp. 41–52, 2011.

[117] H. Grandel, J. Kaslin, J. Ganz, I. Wenzel, and M. Brand, "Neural stem cells and neurogenesis in the adult zebrafish brain: Origin, proliferation dynamics, migration and cell fate," *Dev. Biol.*, vol. 295, no. 1, pp. 263–277, 2006.

[118] A. Arslan-Ergul and M. M. Adams, "Gene expression changes in aging Zebrafish (Danio rerio) brains are sexually dimorphic," *BMC Neurosci.*, vol. 15, 2014.

[119] E. T. Karoglu *et al.*, "Aging alters the molecular dynamics of synapses in a sexually dimorphic pattern in zebrafish (Danio rerio)," *Neurobiol. Aging*, vol. 54, pp. 10–21, 2017.

[120] S. H. Yuan *et al.*, "Cell-surface marker signatures for the Isolation of neural stem cells, glia and neurons derived from human pluripotent stem cells," *PLoS One*, vol. 6, no. 3, 2011.

[121] J. Xu, S. Kobayashi, S. Yamaguchi, K. I. Iijima, K. Okada, and K. Yamashita, "Gender effects on age-related changes in brain structure," *Am. J. Neuroradiol.*, vol. 21, no. 1, pp. 112–118, 2000.

[122] P. M. Lledo, M. Alonso, and M. S. Grubb, "Adult neurogenesis and functional plasticity in neuronal circuits," *Nat. Rev. Neurosci.*, vol. 7, no. 3, pp. 179–193, 2006.

[123] I. Ferrer, "Diversity of astroglial responses across human neurodegenerative disorders and brain aging," *Brain Pathol.*, vol. 27, no. 5, pp. 645–674, 2017.

[124] R. R. Voskuhl *et al.*, "Reactive Astrocytes Form Scar-Like Perivascular Barriers to Leukocytes during Adaptive Immune Inflammation of the CNS," *J.*